Light Water Reactor Sustainability Program

Safety Analysis of FeCrAl Accident-Tolerant Fuels with Increased Enrichment and Extended Burnup for PWR

September 2023

U.S. Department of Energy

Office of Nuclear Energy

Safety Analysis of FeCrAl Accident-Tolerant Fuels with Increased Enrichment and Extended Burnup

Yong-Joon Choi
Idaho National Laboratory

Abe Whitmeyer
Kenneth Franzese
Ben Lindley
University of Wisconsin-Madison

September 2023

Idaho National Laboratory
Light Water Reactor Sustainability
Idaho Falls, Idaho 83415

Page intentionally left blank

EXECUTIVE SUMMARY

The U.S. nuclear industry is facing a strong challenge to maintain regulatory-required levels of safety while ensuring economic competitiveness to stay in business. Safety remains a key parameter for all aspects related to the operation of light water reactor nuclear power plants (NPPs), and it can be achieved more economically by using a risk-informed ecosystem, such as that being developed by the Risk-Informed Systems Analysis Pathway under the U.S. Department of Energy Light Water Reactor Sustainability Program. This program is promoting a wide range of research and development activities to maximize both the safety and economically efficient performance of NPPs through improved scientific understanding, especially given that many plants are considering a second license renewal.

The Risk-Informed Systems Analysis Pathway has two main goals:

- The deployment of methodologies and technologies that enable a better representation of the safety margins and factors that contribute to cost and safety

- The development of advanced applications that enable cost-effective plant operation.

As part of this pathway, the Enhanced Resilient Plant project refers to an NPP where safety is improved by implementing various measures, such as accident-tolerant fuels, diverse and flexible coping strategies, enhancements to plant components and systems, incorporation of augmented or new passive cooling systems, and utilization of advanced battery technologies. The objective of the Enhanced Resilient Plant project is to use novel methods and computational tools to enhance existing reactors' safety while reducing operational costs.

This report documents research and development conducted in support of deployment of accident-tolerant fuels. This project performed safety analyses for the steady-state normal operation, anticipated operational occurrences, and design-basis accidents of a representative four-loop pressurized water reactor model with Zr and FeCrAl accident-tolerant fuel clad with higher enrichment and burnup supporting plant refueling cycles of 18 and 24 months. The source terms and environmental impacts were studied for a large-break loss of coolant accident, including uncertainty analyses.

Page intentionally left blank

CONTENTS

FIGURES

TABLES

ACRONYMS

AFW	auxiliary feedwater
ANS	American Nuclear Society
AOO	anticipated operational occurrences
ATF	accident-tolerant fuels
BDBA	beyond design-basis accident
CHF	critical heat flux
CVCS	chemical and volume control system
DBA	design-basis accident
DNBR	departure of nucleate boiling ratio
ECCS	emergency core cooling system
ERP	Enhanced Resilient Plant
FFRD	fuel fragmentation, relocation and dispersal
FSAR	final safety analysis report
FY	fiscal year
HBU	high burnup
HPSI	high-pressure safety injection
INL	Idaho National Laboratory
LBLOCA	large-break loss of coolant accident
LOCA	loss of coolant accident
LPSI	low-pressure safety injection
LWR	light water reactor
MACCS	MELCOR Accident Consequence Code System
MFW	main feedwater
MSLB	main steam line break
NPP	nuclear power plant
NRC	U.S. Nuclear Regulatory Commission
PCT	peak cladding temperature
PRZ	pressurizer
PWR	pressurized water reactor
RAVEN	Risk Analysis Virtual ENvironment
RCCA	rod cluster control assembly
RCP	reactor coolant pump
RCPB	reactor coolant pressure boundary

RCS	reactor coolant system
RHRS	residual heat removal system
RPV	reactor pressure vessel
RWS	refueling water storage
SBLOCA	small-break loss of coolant accident
SG	steam generator
SGTR	steam generator tube rupture
SOARCA	state-of-the-art reactor consequence analyses
TEDE	total effective dose equivalent
WABA	wet annular burnable absorber
WBN	Watts Bar nuclear power plant

1. INTRODUCTION

The U.S. Department of Energy's Light Water Reactor Sustainability Program, Risk-Informed Systems Analysis Pathway, Enhanced Resilient Plant (ERP) project aims to enhance both the safety and economics of existing nuclear power plants (NPPs) using advanced, near-term technologies that provide substantial improvements to plant safety margins. The project supports the Department of Energy and industry initiatives targeting improvements in the safety and economic performance of the current fleet of NPPs, such as accident-tolerant fuels (ATFs), diverse and flexible coping strategies, passive cooling system designs, and advanced battery technologies. The ERP concept refers to an NPP where safety is improved by implementing various measures, such as those described in the previous sentence. The objective of the ERP research is to use novel methods and computational tools to enhance existing reactors' safety while reducing operational costs. From fiscal year (FY) 2022, the project is focusing on the safety assessments of ATFs with increased enrichment and extended burnup (i.e., high burnup [HBU]), which is an urgent near-term industry initiative that offers safety enhancements as well as economic gains. [1] This work could serve as a roadmap for safety analyses that NPPs must include in their license amendment requests supporting the use of ATFs.

The possibility of higher burnup is more achievable with ATF compared to the traditional Zr clad fuel due to ATF's more robust cladding properties to cope with accident conditions. In this context, extended HBU operation up to 24 months can provide a significant economic benefit for operating nuclear reactors. However, ATF development is still ongoing along with the enhancement of the modeling and simulation capabilities that can provide sufficient information about how HBU ATF performs under accident scenarios. The safety analyses of HBU ATF are still incomplete, especially in terms of fuel performance. The fuel cladding failure could occur during postulated accident events and may cause fuel damage exceeding the regulation safety limits. The main limiting degradation phenomena are the cladding deformation and fuel fragmentation, relocation, and dispersal (FFRD). Cladding deformation is possible during a loss of coolant accident (LOCA).

FY-2023 research focused on the safety analysis of ATF with increased enrichment for the higher burnup fuel cycle operation. The safety analyses include steady-state normal operation, anticipated operational occurrences (AOOs), design-basis accidents (DBAs), and beyond DBAs (BDBAs; e.g., severe accident) addressed in NUREG-0800, "Standard Review Plan for the Review of Safety Analysis Reports for Nuclear Power Plants: LWR Edition." [2] The project also performed a consequence analysis from released radioactivity across the engineered safety boundary and to the environment. The consequence analyses support understanding changes between the conventional Zr clad fuels as related to NUREG-1465[3], which was developed for the conventional Zr clad fuel with lower burnup, and ATF-clad fuels. This work could serve as a roadmap or reference for safety and consequence analyses that NPPs must include in their license amendment requests for an HBU fuel cycle operation.

The main activities in FY-2023 are:

- An assessment of modeling and simulation technical gaps in the safety analysis of HBU ATFs by using the Idaho National Laboratory (INL) developed thermal-hydraulic code RELAP5-3D, focusing on capabilities in assessing the FFRD phenomenon. [4]

- Safety analyses of a pressurized water reactor (PWR) loaded with ATF with extended burnup cycles of 18 and 24 months for normal operation, AOOs, DBAs and BDBA initiated by a recovered[1] large-break LOCA (LBLOCA).

- Source term and environmental impact analyses from recovered LBLOCA in a PWR with highly enriched Zr and ATF-clad fuel with extended burnup cycles of 18 and 24 months including uncertainty analysis.

---

[1] Recovered LBLOCA is the standard severe accident scenario of the U.S. NRC case study that intentionally delays emergency core cooling system (ECCS) during an LBLOCA to lead reactor core and fuel damage. [7]

1.1   Accident Scenarios for Safety Analysis

1.1.1   Design-Basis Accidents

Safety analyses were performed for an ATF-loaded HBU operation PWR based on DBAs in NUREG-0800. [2] The selection of DBAs was based on the U.S. Nuclear Regulatory Commission (NRC) and American Nuclear Society (ANS) guidance. [5][6] Four different conditions are proposed for consideration in the safety analysis report. The entire list of accidents is given in Appendix A, and a total of five DBA scenarios were selected. The following is the list of conditions and representative accidents included in this project.

- Condition I—Normal Operation and Operational Transients were not simulated in this study, as the steady-state normal operation was simulated instead.

- Condition II—Faults of Moderate Frequency (i.e., AOO).

  - Turbine trip

- Condition III—Infrequent Faults

  - LOCAs resulting from a spectrum of postulated piping breaks within the reactor coolant pressure boundary (RCPB) (e.g., small-break LOCA [SBLOCA])

- Condition IV—Limiting Faults

  - Steam system piping failure (major)

  - Steam generator (SG) tube failure

  - LOCAs resulting from the spectrum of postulated piping breaks within the RCPB (e.g., LBLOCA).

The main parameters of interest from the safety analysis were selected based on the thermophysical phenomena of the specific accident, including the departure of nucleate boiling ratio (DNBR), peak cladding temperature (PCT), fuel failure (e.g., rupture) occurrences, and hydrogen generation and cladding oxidation behavior if applicable.

1.1.2   Beyond Design-Basis Accident

For the BDBA analysis, the consequence analysis was performed based on the U.S. NRC's State-of-the-Art Reactor Consequence Analyses (SOARCA) project, which analyzed source terms and environmental impact due to a severe accident caused by a recovered LBLOCA. [7] The major radioactive isotopes were evaluated based on NUREG-1465. [3]

The consequence analysis includes short- and long-term exposure and health impacts, dose to the environment, and economic impacts from the protective and remediation actions.

The regulatory guidelines of the source term are given in, 10 CFR 50.67, "Accident Source Term," as [8]:

 i. An individual located at any point on the boundary of the exclusion area for any 2 hours following the onset of the postulated fission product release, would not receive a radiation dose in excess of 0.25 Sv (25 rem) total effective dose equivalent (TEDE).

 ii. An individual located at any point on the outer boundary of the low population zone, who is exposed to the radioactive cloud resulting from the postulated fission product release (during the entire period of its passage), would not receive a radiation dose in excess of 0.25 Sv (25 rem) TEDE.

 iii. Adequate radiation protection is provided to permit access to and occupancy of the control room under accident conditions without personnel receiving radiation exposures in excess of 0.05 Sv (5 rem) TEDE for the duration of the accident.

The above terms should be evaluated from the applicable DBA as a consequence analysis in the safety analysis report. The amount of fission product release should be assumed from a major accident, (i.e., substantial meltdown of the core due to a postulated accident). It is also noted that 0.25 Sv TEDE is not an

absolute acceptable limit for the emergency dose to the public under accident conditions. It is a reference value that can be used in the evaluation of proposed design-basis changes with respect to potential reactor accidents of exceedingly low probability and low risk of public radiation exposure. The acute radiation syndrome limit is 0.7 Sv. [3]

2.   STEADY-STATE NORMAL OPERATION MODELING

2.1   Model Description

The RELAP5-3D four-loop Westinghouse PWR model was developed based on the Zion NPP. This model was originally used for a system safety feedback effect in the Plant Reload Optimization project in the Risk-Informed Systems Analysis Pathway. [9] The model has been fully validated by steady-state and various transient calculations. For this project, the model has been updated to reflect the change in plant configuration (e.g., HBU power history) and to be compatible with the ATFs and other design-basis and severe accident scenarios.

Figure 1 shows the sample nodalization of four-loop Westinghouse PWR for RELAP5-3D analysis, which has better visibility[2].
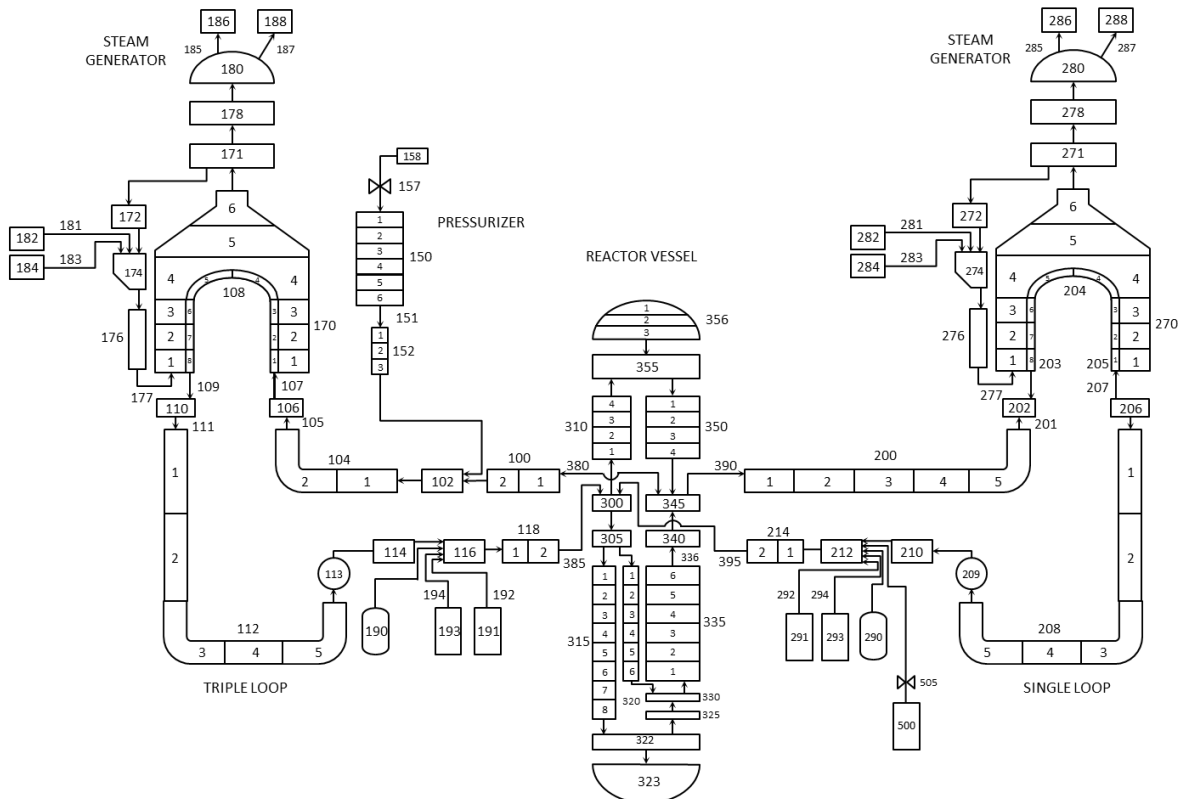
Figure 1. Sample RELAP5-3D nodalization for four-loop Westinghouse PWR.

The model has a total of 188 hydraulic volumes connected with 199 junctions, coupled with 25 heat structures to simulate heat generation and loss. Two reactor core channels were modeled for the average and hottest core power area, representing a total of 193 fuel assemblies. The hottest core power area was used to evaluate the fuel failure during the transient. The reactor core bypass (i.e., downcomer or belt line region) and lower and upper plenum are modeled with no heat losses toward the containment, thus adiabatic. The reactor core is linked with four identical SG loops with one loop to be transformed into the "broken loop" during LOCA. The point reactor kinetics model was used for the reactor power controlling during normal operation. The cladding and fuel geometry (e.g., cladding thickness, cladding surface characteristics, inner pressure) and moderator temperature reactivity feedback coefficients were assumed to be identical in both Zr and ATF cases.

---

[2] The original model was developed by SNAP software and is shown in Appendix B.

The following components are modeled:

- Reactor pressure vessel (RPV)

- Four coolant loops including four coolant pumps and four SGs

- One pressurizer (PRZ) and its main valves (i.e., PORV and SV[3])

- Connections for the emergency core cooling system (ECCS) and auxiliary feed water system (AFWS)

- A secondary part of the SGs up to the SG outlet, including the SG main valves (i.e., PORV and SV)

- Main and auxiliary feedwater (MFW and AFW) systems as system boundary conditions

- ECCS includes high- and low-pressure safety injection (HPSI and LPSI) systems and accumulators

- Other modeling limitations and assumptions were given in Reference [9].

The possible operator actions (SG cool down, feed and bleed, MFW and AFW flow control, HPSI and LPSI actuation, relief valve control, and main steam line control) are implemented through the RELAP5-3D control logic system. RELAP5-3D control variables calculate the derived parameters for the control logic system and transient analysis. Table 1 and Table 2 describe major design parameters and engineered safety features of a four-loop Westinghouse PWR.

Table 1. Major design parameters of four-loop Westinghouse PWR RELAP5-3D model. [10]

Parameter	Value (SI)	Value (Imperial)
Core power [MW_{th}]	3,250	
Nominal system pressure [MPa or psia]	15.5	2250.0
Reactor inlet/outlet temperature [°C or °F]	276.8/312.3	530.2/594.2
Number of fuel rods	39,372	
Number of fuel assemblies	193	
Rod array	15×15	
Active fuel height [m or in.]	3.6576	144.0
Equivalent core diameter [m or in.]	3.3706	132.7
Total core cross-section area [m^2 or ft^2]	8.9243	96.06
Reactor core barrel inner/outer diameter [m or in.]	3.8735	148.0/152.5
Reactor thermal shield inner/outer diameter [m or in.]	4.0259/4.1656	158.5/164.0
RCS coolant flow [kg/s or lbm/hr]	17,009.7	135.0E+6
Heat flux hot channel factor, F_Q	2.4~2.55	
Nuclear enthalpy rise hot channel factor, $F^N_{\Delta H}$	1.59~1.65	
Minimum DNBR[4] in typical flow channel	2.53	

[3] PORV: Pilot-operated relief valve and SV: Safety valve.

[4] Departure from nucleate boiling ratio

Parameter	Value (SI)	Value (Imperial)
RPV design/operating pressure [MPa or psia]	17.1/15.4	2,485/2,235
RPV design temperature [°C or °F]	343.3	650
Overall height of RPV and closure head [m or in.]	1.1/0.8	43.4/32
Thickness of RPV insulation [m or in.]	0.0762	3
Number of SGs	4	
SG design pressure, reactor coolant/steam [MPa or psig]	17.1/7.4	2485/1085
SG design temperature, reactor coolant/steam [°C or °F]	343.3/315.6	650/600
SG total heat transfer surface area [m^2 or ft^2]	4784.5	51,500
Number of SG U-tubes	3,388	
Outer diameter of SG U-tube [m or in.]	0.022	0.875

Table 2. Major engineered safety features of four-loop Westinghouse PWR RELAP5-3D model. [10]

Parameter	Value (SI)	Value (Imperial)
Number of accumulators	4	
Accumulator water volume [m^3 or ft^3]	38.2	1350 each
Accumulator operation temperature [°C or °F]	37.8~65.6	100~150
Accumulator operation pressure [MPa or psig]	4.137~4.482	600~650
RWS[5] tank/required capability [l or gal]	1,472,525/1,324,894	389,000/350,000
RWS operation temperature [°C or °F]	4.4~37.8	40~100
RWS operation pressure [MPa or psig]	0.1	14.7
ECCS charging pump capacity [m^3/s or gpm]	2×0.009(at 1,767 m)	2×150 (at 5,800 ft)
ECCS safety injection pump capacity [m^3/s or gpm]	2×0.025(at 762 m)	2×400 (at 2,500 ft)
Residual heat removal pump capacity [m^3/s or gpm]	2×0.189(at 107 m)	$2 \times 3,000$ (at 350 ft)
Boron injection tank volume [l or gal]	3406.87	900.0
Boron concentration [wt%]	11.5 ~ 13.0	
AFW pump motor/turbine driven capacity [m^3/s or gpm]	$2 \times 0.031/1 \times 0.062$	$2 \times 495/1 \times 990$

[5] Refueling water storage

2.2 Specific RELAP5-3D Modeling for Accident-Tolerant Fuel and High Burnup Technologies

2.2.1 Power History for Decay Data

For reactor kinetics, RELAP5-3D has the option of implementing the energy from the fission product decay heat and actinide quantities based on reactor operation power history. The power history option can include operational and irregular fuel reloading cycle periods of NPPs. For each input period, the input consists of the total power, the time duration at that power, and the fraction of power from major actinides (e.g., ^{235}U, ^{238}U, ^{239}Pu, and ^{241}Pu). The decay heat is calculated from the ANS standard decay heat model from an LWR, which was set in RELAP5-3D modeling data. [6] Data from the 1979, 1994, and 2005 editions are available. More detail is available in the RELAP5-3D manual. [11]

Table 3 shows the amount of decay power calculated based on the 1979 ANS standard decay heat model from an LWR, which was set in a RELAP5-3D model and compared with ANS data and a SCALE code simulation. RELAP5-3D slightly overpredicts the decay power compared to reference values.

Table 3. Decay power prediction of 3,411 MWth normal operation power.

Burnup Length and Fuel	ANS-1979	SCALE	RELAP5-3D
Zr clad fuel with 18 months	2.193028E+8	2.0965710E+8	2.2983654E+8
FeCrAl clad fuel with 18 months	2.193296E+8	2.1178902E+8	2.2983654E+8
FeCrAl clad fuel with 24 months	2.195407E+8	2.1222468E+8	2.2999423E+8

2.2.2 Metal-Water Reaction

The RELAP5-3D metal-water reaction model was used to simulate cladding oxidation and hydrogen generation. Table 4 shows parameters used for both the Zr and FeCrAl oxidation model. A monolithic metal-water reaction model was used for FeCrAl instead of using the temperature transition threshold model. [12] Cladding thickness was assumed identical in both Zr and FeCrAl cases.

Table 4. RELAP5-3D parameters for cladding oxidation modeling. [12]

Parameter	Zr	FeCrAl
Reaction rate constant [m^2 metal/s]	9.166E-7	2.444E-5
Reaction heat release [J/kg mole]	5.94E+8	6.73E+7
Activation energy [cal/model]	35,890	82,218
Density [kg/m^3]	6,500	6,860
Molecular weight [kg/kg mole]	91.22	53.96
Molecular weight reactant/clad ratio	0.0442	0.112
Initial fuel cladding gap pressure [MPa]	6.8947	6.8947
Fuel surface roughness [m]	1.E-6	1.E-6
Cladding surface roughness [m]	2.E-6	2.E-6
Cladding thickness [mm]	0.1524	0.1524

2.2.3 Cladding Deformation Model

The RELAP5-3D model has been taken from the FRAP-T6 code and was used in current research to evaluate fuel failure during accidents. [11] The purpose of the model is to take into account a possible plastic deformation of the cladding during an accidental condition. The model can inform the user of a possible clad rupture and ballooning and of a possible flow blockage due to the hydraulic channel flow area reduction. The fuel failure model used in RELAP5-3D was found to be highly conservative compared to the experimental data. [4] Currently, only the Zr cladding fuel failure model is available in RELAP5-3D and was used for the ATF cladding fuel failure model in this study. Further investigation by specialized fuel pin mechanics codes are needed if extensive plastic deformation or cladding rupture is detected.

2.3 Result of Steady-State Normal Operation with Accident-Tolerant Fuel and High Burnup

A steady-state simulation was performed to verify the developed RELAP5-3D model is correctly working with ATF and HBU operation. A simulation was performed for 3,000 seconds to allow the model to reach a sufficient steady-state. As shown in Table 5, most of the major design parameters are found within an acceptable range compared to reference values. The total reactor power is the sum of power from fission (i.e., fission from prompt and delayed neutron) and power from decay (i.e., fission product and actinide). Power from fission in a 24-month burnup cycle is lower than the 18-month case. However, power from decay is higher in the 24-month burnup cycle.

No significant discrepancy in the values was found between Zr and FeCrAl ATF and between the 18 and 24-month burnup cycles.

Table 5. Major operational parameters from steady-state normal operation.

Parameter	Reference Value [10]	Zr 18 Month	FeCrAl 18 Month	FeCrAl 24 Month
Total reactor power [W]	3.636E+9 (given)	3.6359984E+9	3.6359962E+9	3.6360001E+9
Power from fission [W]	NA	3.3910012E+9	3.390999E+9	3.3908348E+9
Power from decay [W]	NA	2.4499715E+8	2.4499718E+8	2.4516526E+8
Power from actinides [W]	NA	7.7983084E+6	7.798308E+6	7.7979247E+6
PRZ pressure [MPa]	15.5	15.67~15.36	15.67~15.36	15.67~15.36
RCS coolant loop flow rate [kg/s]	17,009.7	18,030.9	18,031.4	18,031.4
Reactor inlet temperature [°C]	312.3	330.468	330.458	330.458
Reactor outlet temperature [°C]	276.8	264.452	264.433	264.433
DNBR	<2.53	2.09902	2.09919	2.09919

Figure 2 and Figure 3 show the steady-state power level from total reactor power and reactor power from fission from ^{235}U and other actinides, respectively. The higher burnup (i.e., 24 months) fuel cycle case shows a lower fission power compared to the lower burnup (i.e., 18-months) fuel cycle case. The power from other actinides (e.g., ^{238}U, ^{239}Pu, and ^{241}Pu) is smaller in the 24-month case since the amount of fissile material lessens as burnup increases. However, the power from fission products in 24 months is larger than the 18-month case since a longer operation builds a large amount of fission products.

Figure 4 shows decay heat during steady-state operation and transient when the reactor has been tripped. The 24-month higher burnup shows a larger decay heat level since more fission products were generated from

the longer period of operation (e.g., higher burnup) than the 18-month burnup. However, decay heat drops immediately after the reactor is tripped. No large difference was observed between the 18 and 24-month burnup cases.
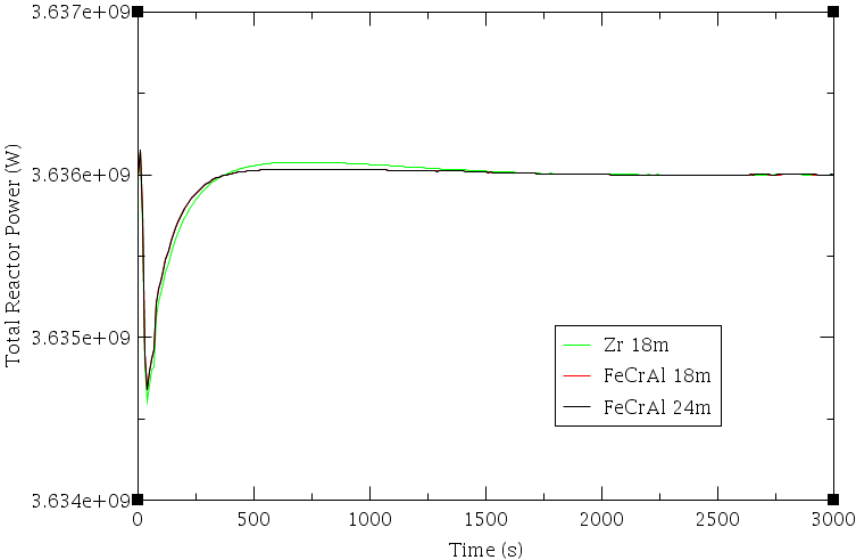
Figure 2. Steady-state total reactor power.
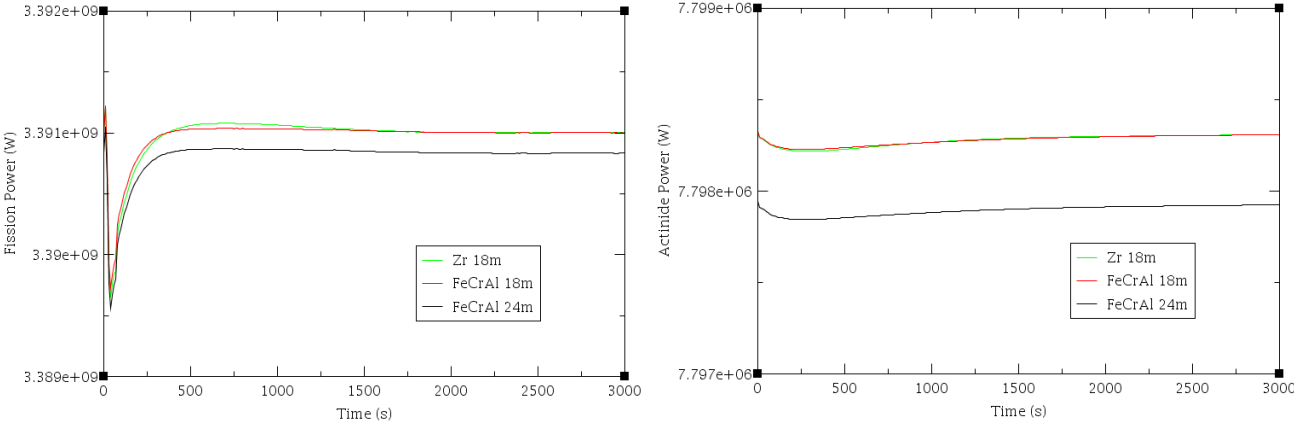
Figure 3. Steady-state reactor power from fission (left) and power from other actinides (right).
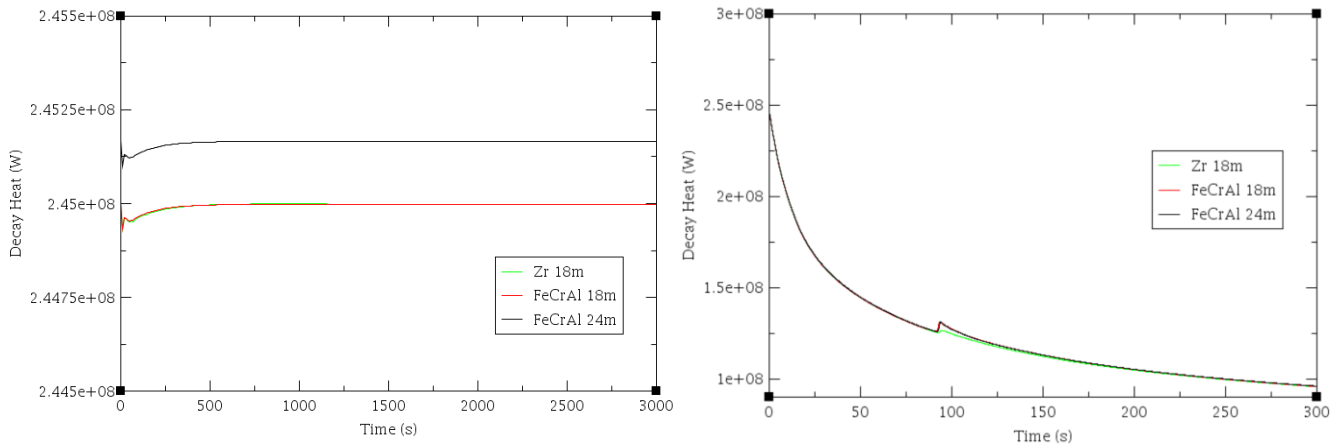
Figure 4. Steady-state (left) and transient decay heat power (e.g., LBLOCA case, right).

Figure 5 shows PCT at steady-state operation. The PCT of Zr cladding was found 663.8 K while FeCrAl cladding showed 648.7 K at 3,000 seconds.
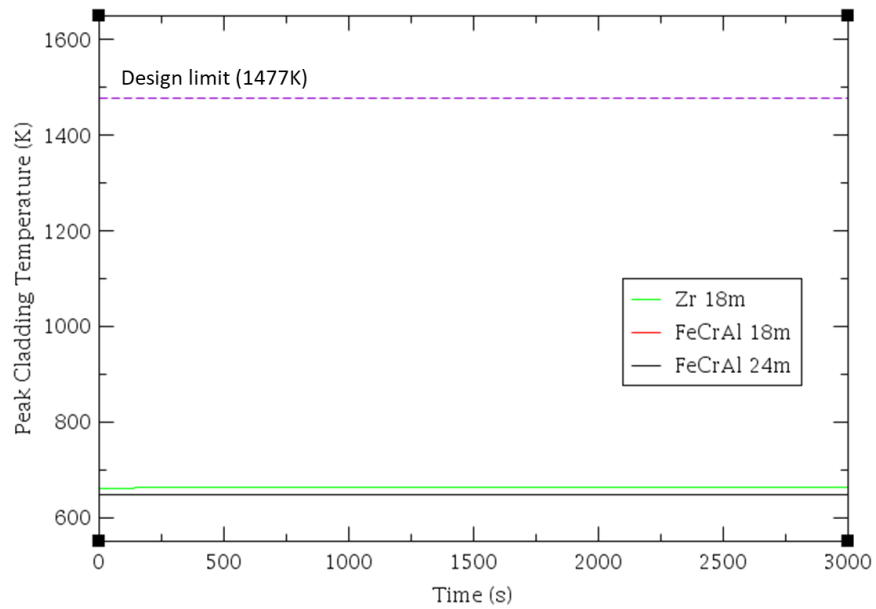
Figure 5. Steady-state PCT.

Figure 6 shows DNBR at a steady-state calculation is near 2.1, which is higher than the operational limitation (e.g., DNBR > 1.2).
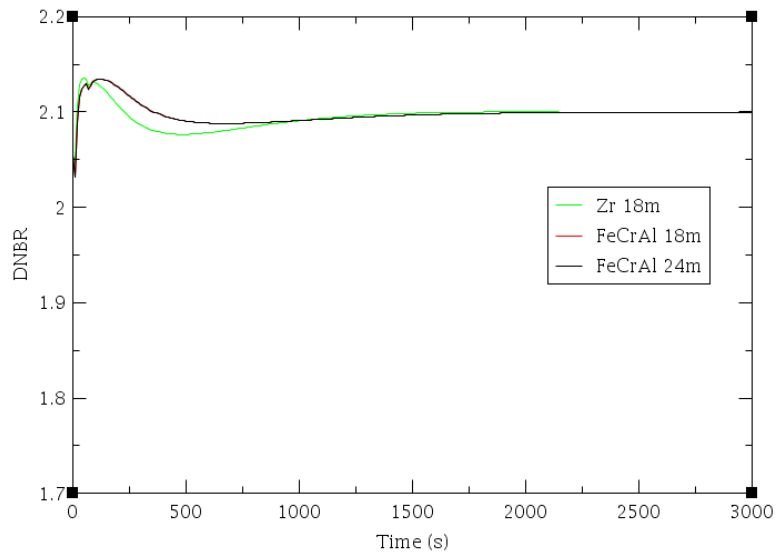
Figure 6. Steady-state DNBR.

No specific issues were observed during the steady-state normal operation analysis.

3.   ANALYSIS OF THE DESIGN-BASIS ACCIDENTS

3.1   Condition II Design-Basis Accidents: Turbine Trip

3.1.1   Problem Description

A turbine trip is classified as a Condition II event and faults moderate frequency. As the turbine trips at the secondary side of the NPP, the reactor trips immediately from a signal derived from the turbine stop signals unless a lower power threshold is allowed. [13] The steam flow to the turbine stops from the immediate closure of the steam feed valve (i.e., turbine stop valve) to block steam flow to the turbine. Since the MFW system remains the same as that of the normal operation, the excessive steam bypasses through the steam dump valve. The loss of steam flow results in a nearly immediate rise of the secondary system temperature and pressure, which also increases the primary reactor coolant system (RCS) temperature and pressure due to a loss of heat removal to the secondary side. The automatic turbine bypass system would accommodate up to 40% of the rated steam flow. Reactor coolant temperatures and pressure do not increase significantly if the turbine bypass and pressure control systems of the PRZ are functioning properly. The bypassed steam is cooled down through the condenser; however, if the condenser is incapable or excess in capability of the condenser, the steam will be released to the environment, which causes a loss of the MFW. In this case, the feedwater flow could be maintained by the AFW system to ensure an adequate decay heat removal capability.

In NUREG-0800, four different turbine trip scenarios are proposed based on the amount of moderator feedback effect and activation of PRZ spray and PORV from the PRZ. In this research, the most conservative case, maximum moderator feedback without PRZ spray and PORV, was simulated to predict the highest influence from the turbine trip to system safety.

The specific input settings for turbine trip simulation are [9]:

- Secondary side steam flow stops at T+0.001 second to model turbine trip

- The main feed water pump flows constantly with 509 kg/sec (1,122.2 lbm/sec)

- Reactor trip signal when the SG water level falls below 8.26 m (27.1 ft)

- No PRZ spray activation

- No PORV during the transient.

3.1.2   Result and Discussion

The coolant liquid level drops as the turbine trips compared to the steady-state, as shown in Figure 7. Figure 8 shows the secondary side average pressure at steady-state and during the transient. Since MFW is constantly activating but steam is blocked from the turbine, the pressure increases at the beginning of the transient but becomes constant by removing heat generated from the reactor via AFW system.

It is noted that data from Zion NPP final safety analysis report (FSAR) is given in the graphs only if data is available.
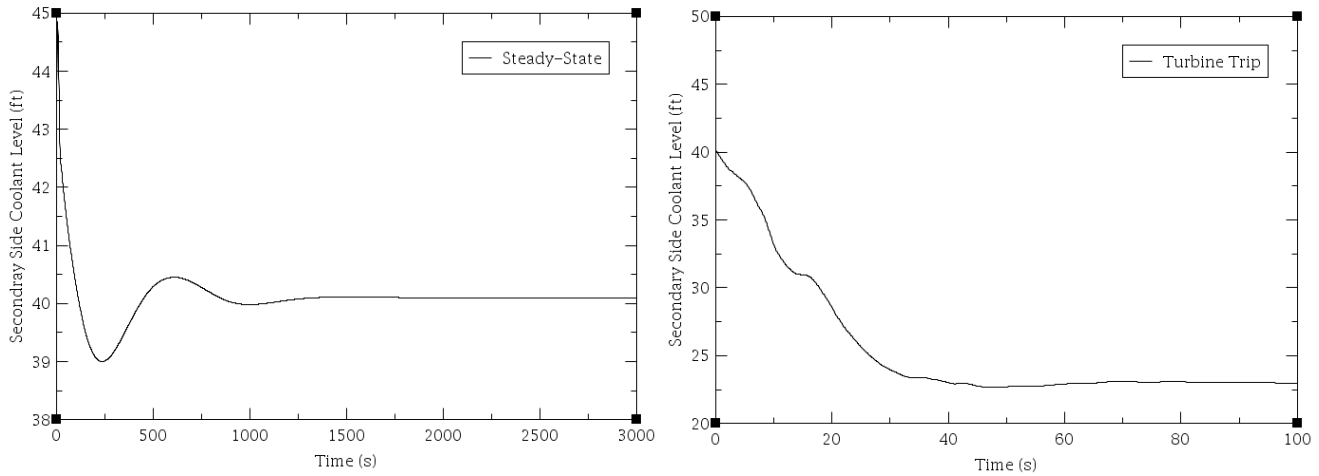
Figure 7. Secondary side coolant liquid level of the steady-state (left) and during the turbine trip (right).
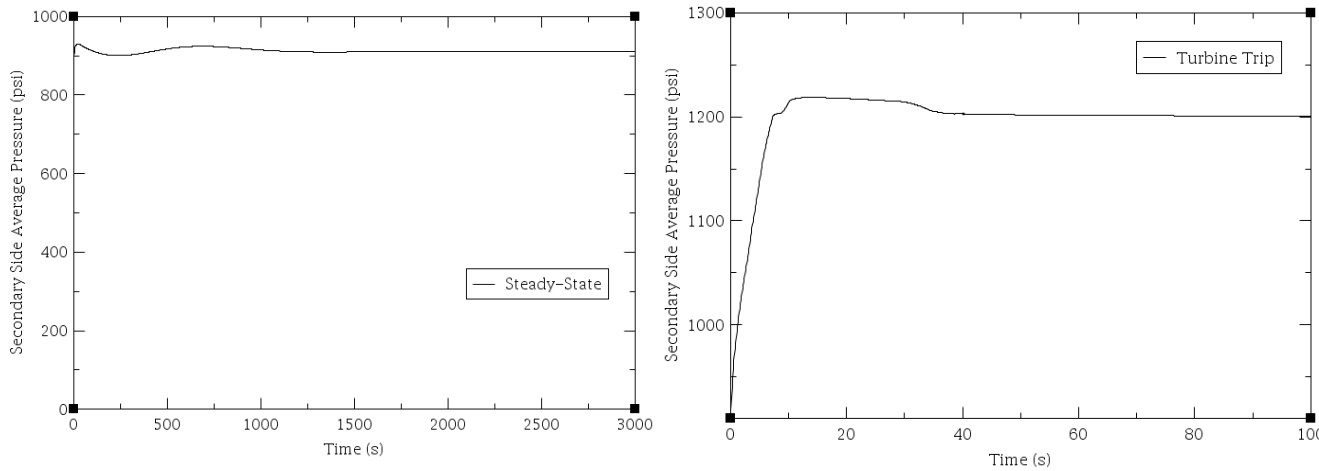
Figure 8. Secondary side average pressure at the steady-state (left) and during the turbine trip (right).

Figure 9 shows the PRZ pressure and average hot leg temperature during a turbine trip. Both pressure and temperature started increasing at the beginning of the transient because heat from the reactor was not properly removed due to the turbine trip. However, once the RCS starts to cool down from the MFW from the secondary side, both pressure and temperature decrease and reach a quasi steady-state level. No large discrepancies were found between the Zr and FeCrAl and 18 and 24-month burnup cases. The results are comparable with the existing analysis in the Zion NPP FSAR. [10] No FSAR data is available for the hot leg average temperature during the turbine trip.
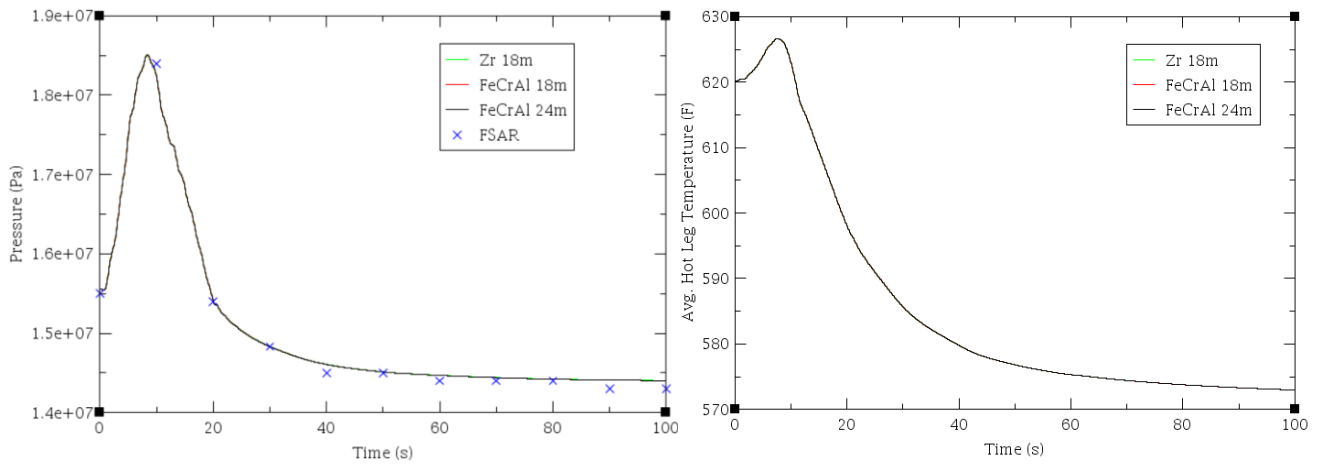
Figure 9. PRZ pressure (left) and hot leg average temperature (right) during turbine trip.

Figure 10 shows the nominal reactor power and Figure 11 shows the PCT during a turbine trip, respectively. The nominal power was in good agreement with the Zion NPP FSAR. [10] However, the PCT of Zr cladding showed a significant rise and drop near the observed steep decrease in nominal power (e.g., T+5 ~ 10 seconds), while FeCrAl clad fuel did not show such behavior. PCT data is not available in Zion NPP FSAR. The main reason is that the Zr cladding starts oxidizing from T+5~10 seconds (e.g., shown in Figure 12), which decreases the heat transfer from fuel cladding to coolant and steeply increases the cladding temperature. This behavior was not shown in FeCrAl cladding cases. However, the PCT did not exceed the design limit (i.e., 1477 K). No fuel failure was observed in this simulation.
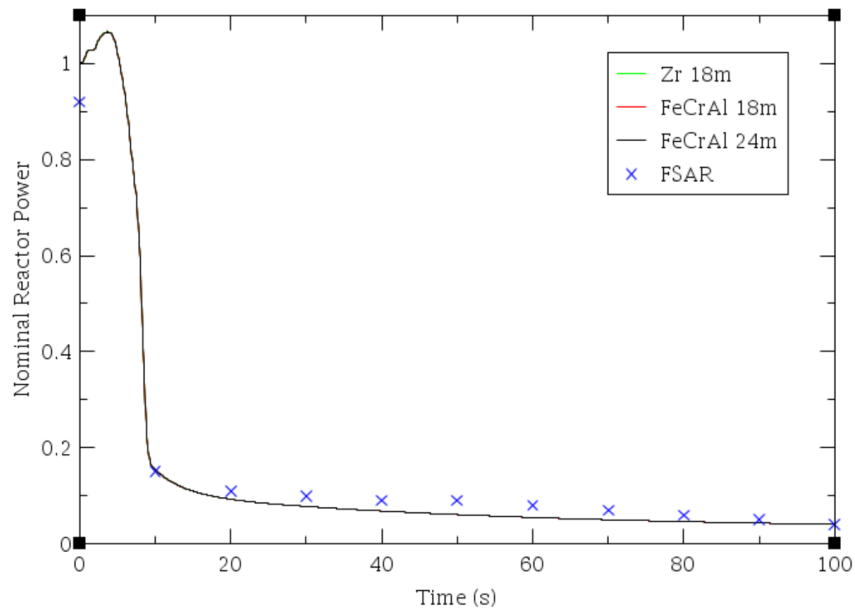
Figure 10. Nominal reactor power during turbine trip.
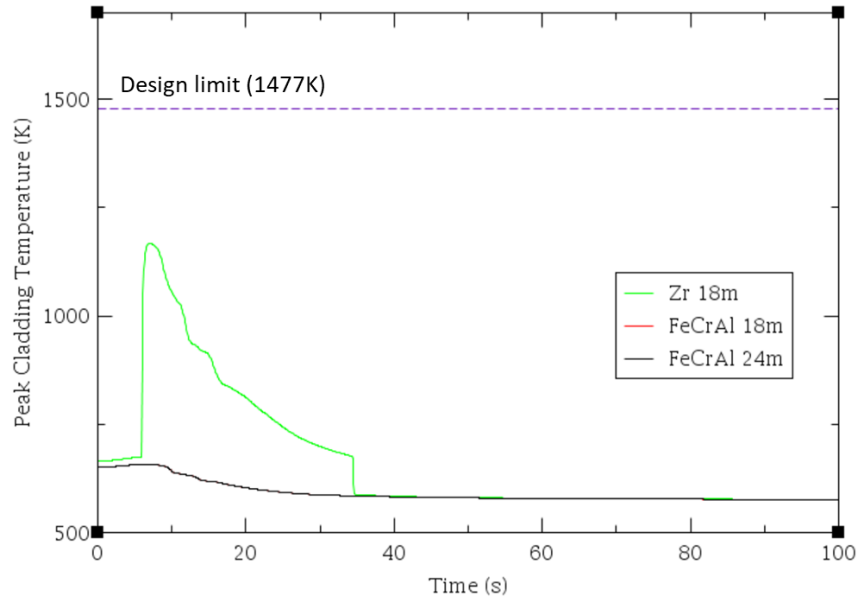
Figure 11. PCT during turbine trip.

Figure 12 shows the amount of generated hydrogen and oxidation rate during a turbine trip. The value from FeCrAl cladding is negligible compared to those of Zr cladding, which is a representative benefit of ATF.
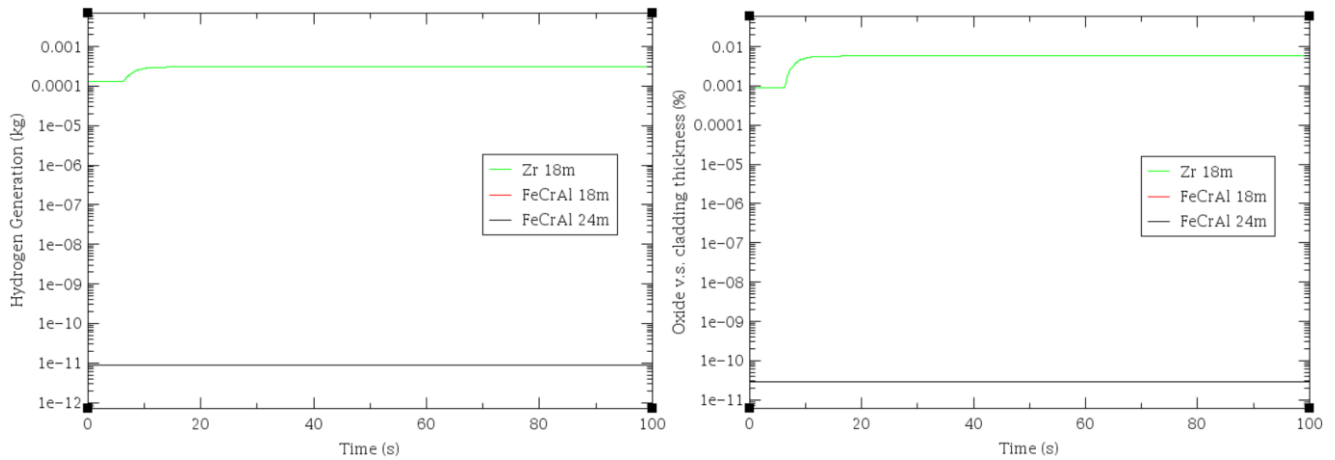
Figure 12. Hydrogen generation amount (left) and oxide vs. cladding thickness (right).

The transient DNBR during a turbine trip is shown in Figure 13. For both Zr and FeCrAl cladding, the DNBR values are increased and dropped to zero. However, the reference value from the Zion NPP FSAR remains constant near a DNBR of 5.0. [10]
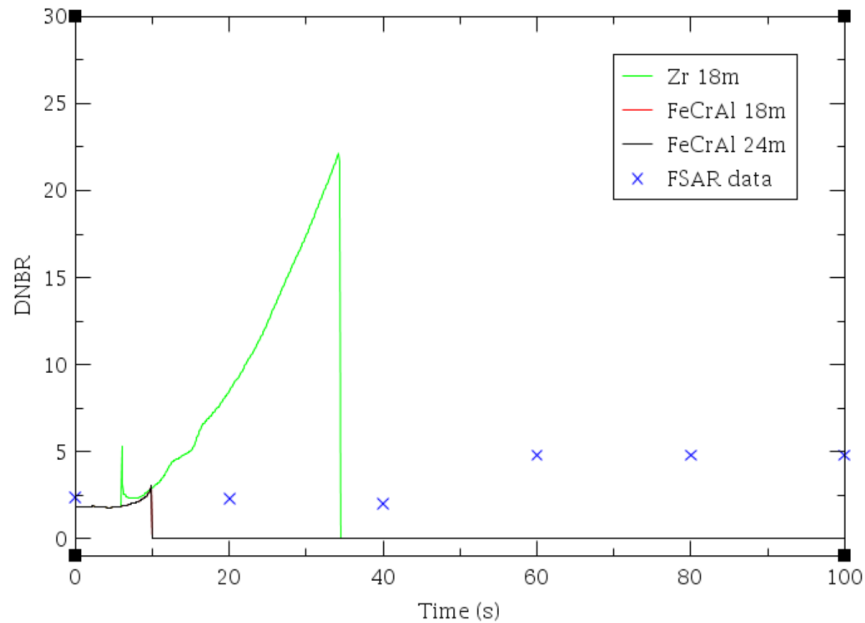
Figure 13. DNBR during turbine trip. [10]

During the simulation of a turbine trip with maximum moderator feedback without PRZ spray and PORV, two issues were observed for Zr cladding with an 18-month burnup cycle. Both PCT and DNBR showed a steep increase and drop where the pressure and reactor power occurred. The main reason was that the initiation of Zr cladding oxidation immediately dropped the heat transfer rate from the cladding to the coolant, which led to a large increase in the PCT and DNBR. However, ATF builds negligible oxidation layer which remain lower value of PCT and DNBR. Another issue is that RELAP5-3D modeling does not correctly predict DNBR compared to Zion NPP FSAR. [10] The reason could be that the given RELAP5-3D model does not correctly represent the local boiling effect in the reactor. Further investigation should include a reactor coolant subchannel analysis.

3.2 Condition III Design-Basis Accidents: Small-Break Loss of Coolant Accident

3.2.1 Problem Description

A LOCA resulting from a spectrum of postulated piping breaks within RCPB is classified as a Condition III event and has an infrequent frequency. This accident is also called a SBLOCA. In this condition, a normally operating reactor coolant pump (RCP) charging system is insufficient to maintain the primary RCS in a normal pressure and PRZ water level.

The main difference between small- and large-break LOCAs is the timeframe of the RCS coolant and pressure discharge through the break. In general, an SBLOCA has a longer period of transition (e.g., tens of minutes to several hours) than an LBLOCA (e.g., seconds to minutes). After a small-break occurs, the primary RCS can maintain a relatively high-pressure and the core remains covered. The pump and reactor trip immediately after a break occurs. The reactor only produces core decay power. The natural circulation by gravitational forces in the RCS is the main driver of removing the heat from the reactor during a SBLOCA, while LBLOCA is dominated by inertial effects from the rapid coolant discharge. The ECCS activates based on the safety injection signals.

The accident sequence is strongly dependent on the location, shape, and size of the break. If the break size is smaller than 9.525 mm (3/8 in.), the RCS does not depressurize because the RCP charging flow can replace the loss of coolant and the HPSI will not be activated. If a break is sufficiently large, the safety injection signal will be alarmed for the HPSI activation. This sufficiently large size is the SBLOCA limiting break, which activates

28

the HPSI, but the RCS pressure does not depressurize rapidly to the accumulator activation point. For a generic Westinghouse PWR, the limiting breaks are typically 5–10 cm (2–4 in.). [14]

The major specific input settings for SBLOCA simulation are [9]:

- Break size set to 6.5 cm^2 (0.007 ft^2)

- Reactor trip at PRZ pressure drops below 13.0 MPa (1,884.7 psia)

- RCP trip T + 0.1 second from reactor trip

- Safety injection delay time was set to T + 40 seconds

- The accumulator activates when PRZ pressure drops below 4.2147 MPa (611.3 psia)

- Low steam pressure safety injection signal 5.5 MPa (100 psia)

3.2.2   Results and Discussion

Figure 14 shows the PRZ pressure and reactor coolant level. The RCS pressure depressurizes slowly as flow is lost through the break until reaching a quasi-steady-state after T + 2,000 seconds, which is comparable to the Zion NPP FSAR. [10] The level of reactor coolant does not change significantly from the top full level. No discrepancy was observed between 18 and 24-month burnups and Zr and FeCrAl cases.
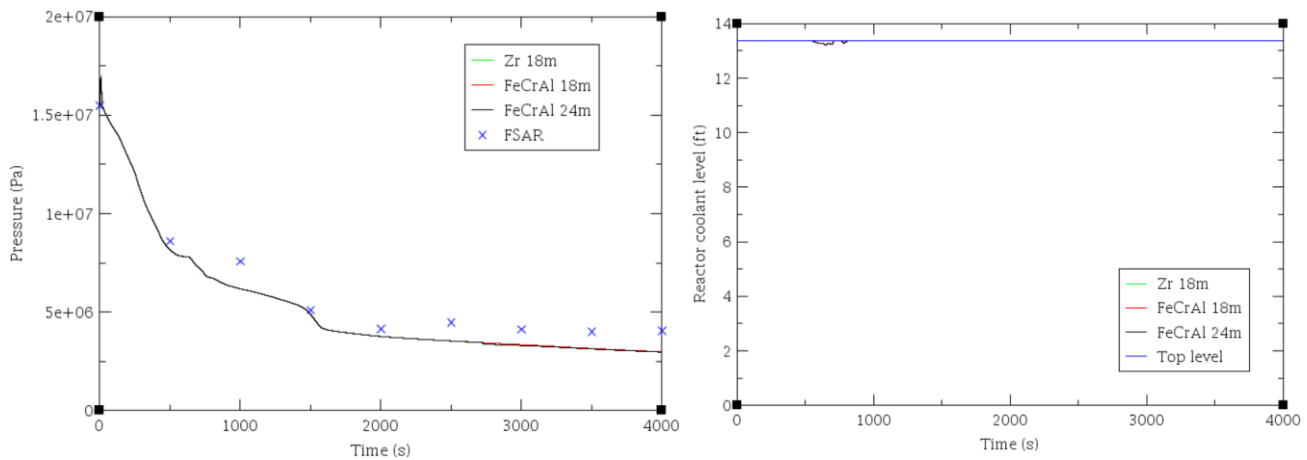
Figure 14. PRZ pressure (left) and reactor coolant level (right) during SBLOCA.

Figure 15 shows the nominal reactor power and hot leg average temperature during an SBLOCA. The power rate dropped to the level of decay heat as soon as the reactor tripped. No Zion NPP FSAR data is available for the comparison.
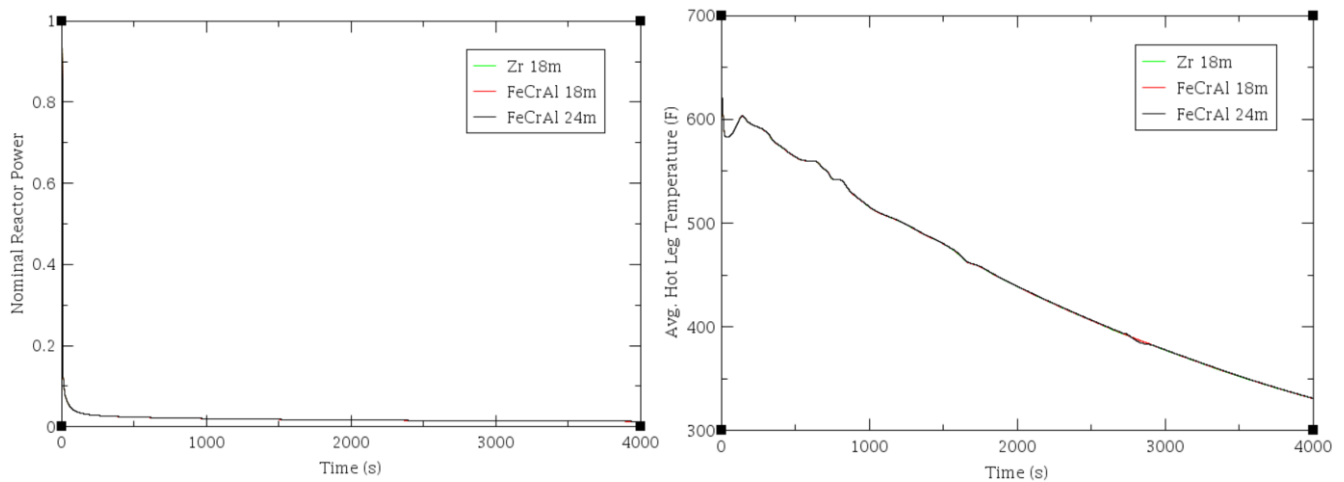
Figure 15. Nominal reactor power (left) and hot leg average temperature (right) during SBLOCA.

Figure 16 shows a PCT during an SBLOCA. No excessive PCT was observed over the design limit in all cases of the simulation since the reactor core is fully covered with coolant and removes decay heat power properly. Fuel failure was not observed throughout the simulation of all cases.

Figure 16. PCT during SBLOCA.

Figure 17 shows the amount of generated hydrogen and oxidation rate during an SBLOCA. The value from the FeCrAl cladding is negligible compared to those of Zr cladding.

Figure 17. Hydrogen generation amount (left) and oxide vs. cladding thickness (right) during SBLOCA.

DNBR during SBLOCA is shown in Figure 18. The values are comparable to FSAR data at the early stage of the accident (e.g., T + 0~8 seconds), which is available data region from Zion NPP FSAR. [10] DNBR calculation data was not produced from RELAP5-3D from T + 12 seconds to T + 300 seconds and from T + 950 seconds until the end of the simulation.

No specific issue was found during the SBLOCA simulation except the DNBR prediction, which was already identified for further investigation.
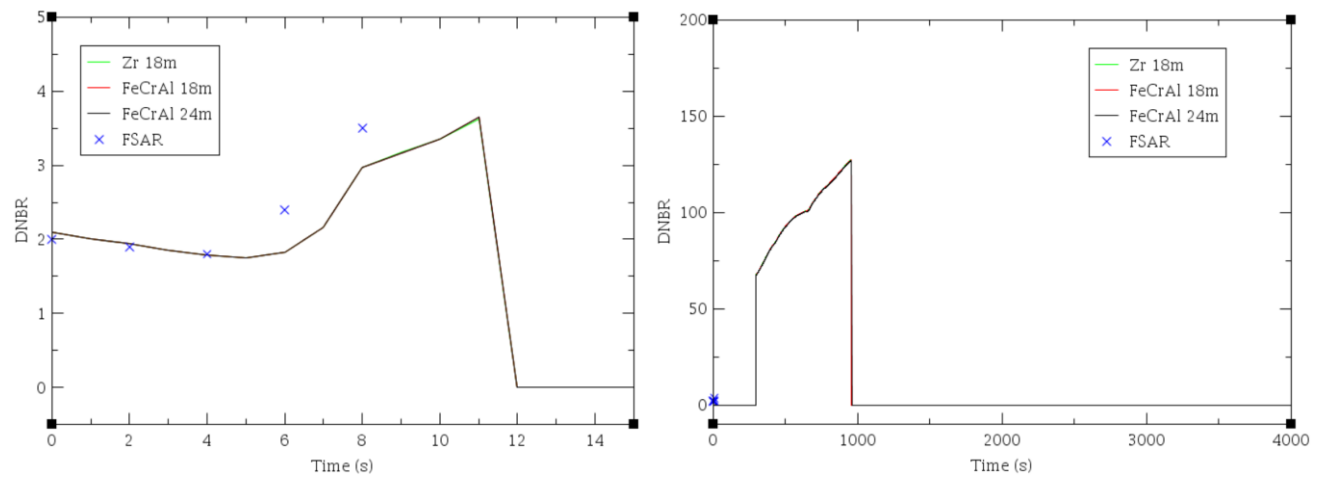
Figure 18. DNBR during SBLOCA over a short (left) and long (right) period. [10]

3.3   Condition IV Design-Basis Accidents: Main Steam System Piping Failure

3.3.1   Problem Description

Steam system piping failure is an ANS Condition IV incident, a limiting fault, and commonly referred to as a main steam line break (MSLB) accident. [5][6]

The steam release arising from a rupture of a main steam line will result in an initial increase in steam flow and decrease during the accident as the steam pressure drops. The energy removal from the RCS causes a reduction of coolant temperature and pressure. In the presence of a negative moderator temperature coefficient, the cooldown results in an insertion of positive reactivity. [15]

One of the major concerns for the MSLB accident is the return of power and criticality in the latter half of the transient. If the most reactive rod cluster control assembly (RCCA) is assumed stuck in its fully withdrawn position after a reactor trip, the core could become critical again and return to generate power. Because of this concern, the MSLB scenario was based on assumptions that conservatively maximize the consequences for a return of power from the accident which occurred during hot full-power operation.

A return of power following a main steam line rupture is a potential problem mainly because of the high-power peaking factors that exist, assuming the most reactive RCCA is stuck in its fully withdrawn position. The core is ultimately shut down by the boric acid solution delivered by the safety injection system and accumulators.

According to NUREG-0800, numerous combinations of break sizes and power levels were run to determine the limiting cases. This study used hot full power operation without an offsite power disturbance case.

The major specific input settings for the MSLB simulation are [9]:

- Steam line break size is 0.074 m^2 (0.8 ft^2)

- Initial steam flow loss is 513.3 kg/sec (1131.6 lbm/sec)

- The reactor trip point was given for T + 23.7 seconds from the transient calculation based on the Zion NPP FSAR [10]

- RCCA stuck delay time was set to T + 8 seconds

- Low steam pressure safety injection signal 5.5 MPa (800 psia)

3.3.2   Results and Discussion

Figure 19 shows nominal reactor power and total steam flow during MSLB. The reactor power increased from the RCCA delay point (i.e., T + 8 seconds) and dropped when the reactor tripped at T + 23.7 seconds until the total shut down of the core. Total steam flow increased due to a loss of heat removal by MSLB and dropped after the reactor is tripped, with a similar trend to the Zion NPP FSAR. [10] No discrepancy was observed between 18 and 24-month burnups and Zr and FeCrAl cases.

Figure 19. Nominal reactor power (left) and nominal total steam flow (right) during MSLB. [10]

Figure 20 shows the RCS pressure and hot leg average temperature behavior during MSLB. No large change was shown in primary RCS loop pressure and temperature due to no coolant loss. Small changes were observed, which followed the RCCA delay (i.e., T + 8 seconds) and reactor trip time (i.e., T + 23.7 seconds). Zr cladding showed slightly higher values, but no significant discrepancy was observed. No Zion NPP FSAR data is available for comparison.
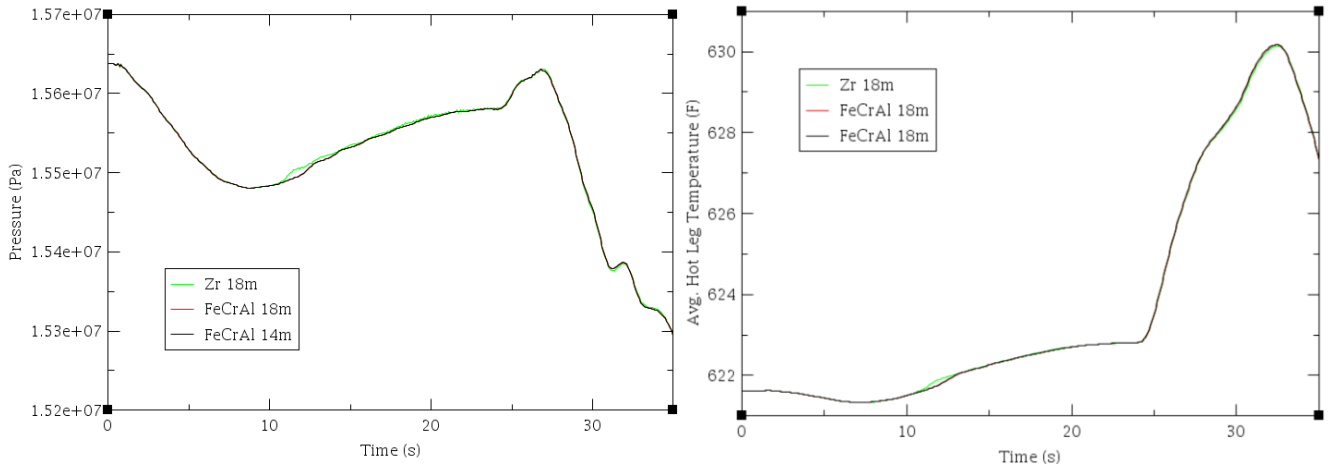
Figure 20. PRZ pressure (left) and hot leg average temperature (right) during MSLB.

Figure 21 shows PCT during a MSLB. Generally, PCT has been increased from the steady-state operation condition but did not show any significant changes during MSLB simulation for both Zr and FeCrAl and 18 and 24-month burnup cases. Fuel failure was not observed throughout the simulation of all cases.
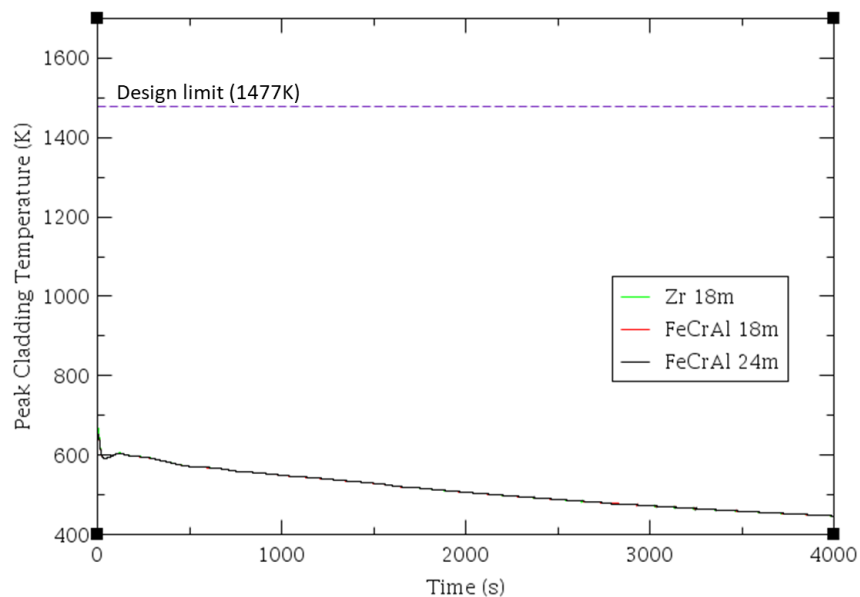

Figure 21. PCT during MSLB.

Figure 22 shows the amount of generated hydrogen and oxidation rate during MSLB. The value from the FeCrAl cladding is negligible compared to those of the Zr cladding.
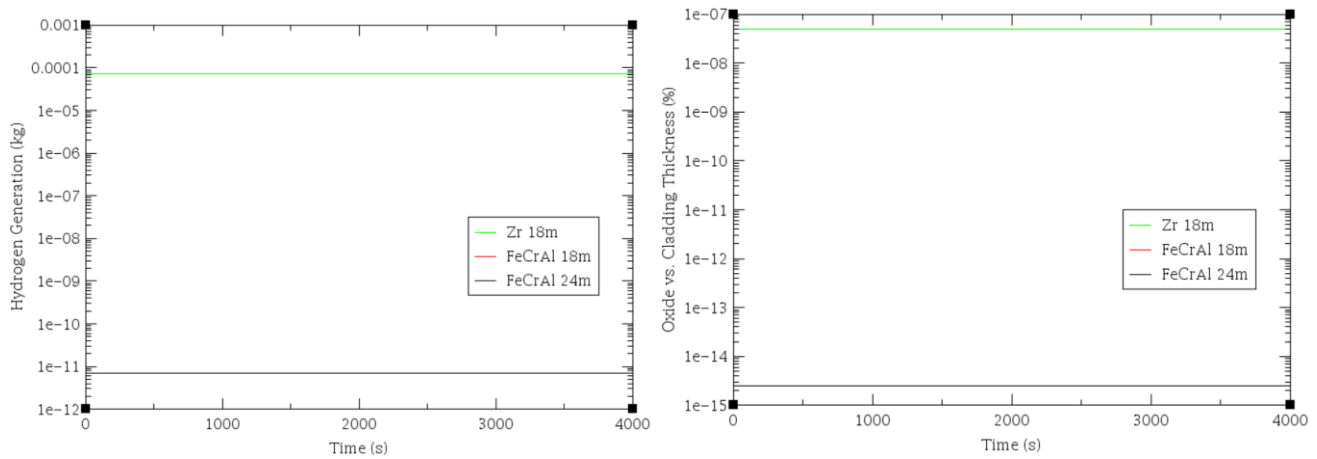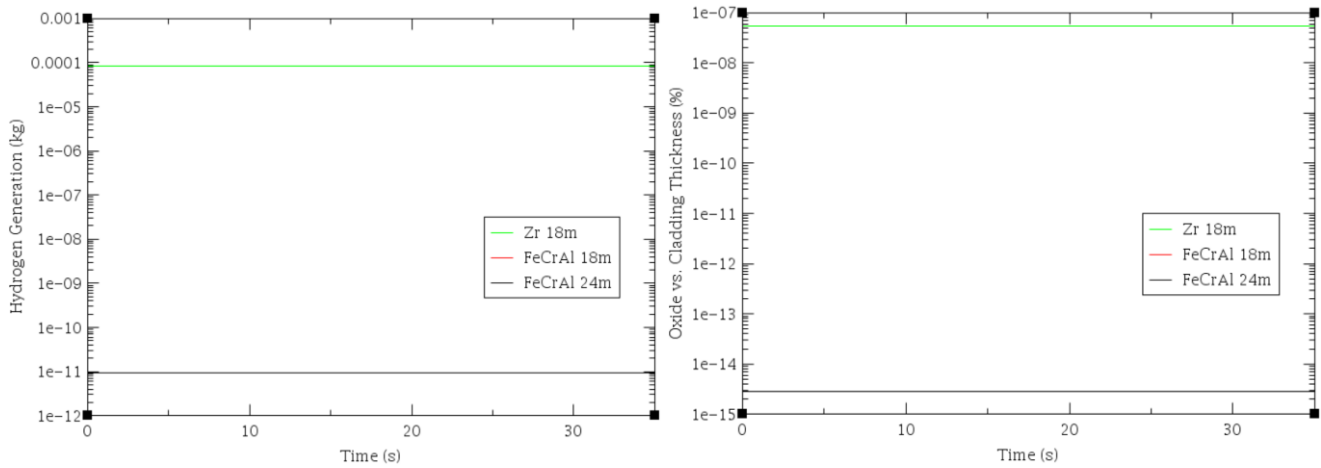
Figure 22. Hydrogen generation amount (left) and oxide vs. cladding thickness (right) during MSLB.

Figure 23 shows the DNBR during MSLB. The values are slightly lower than Zion NPP FSAR, but all values are above the DNBR limitation (e.g., 1.2). [10]

No specific issues were found during the MSLB simulation.
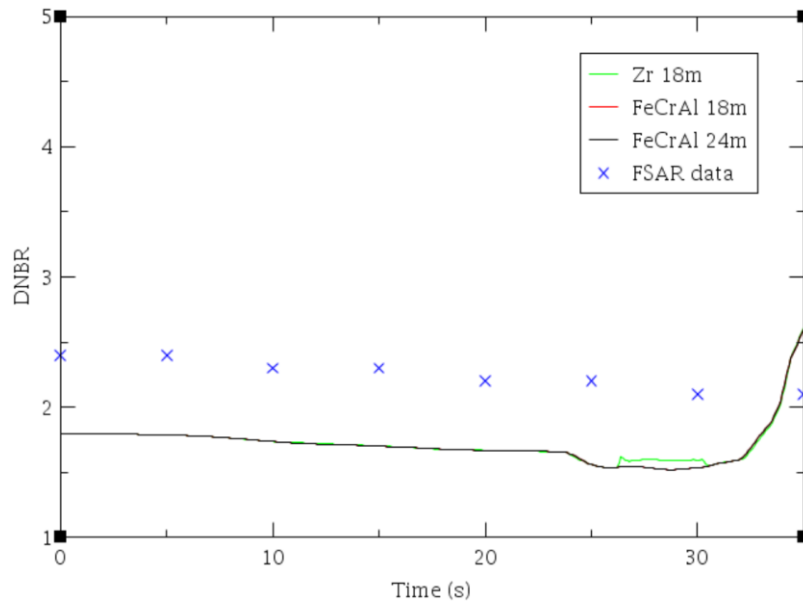
Figure 23. DNBR during MSLB. [10]

3.4 Condition IV Design-Basis Accidents: Steam Generator Tube Rupture

3.4.1 Problem Description

The steam generator tube rupture (SGTR) is an ANS Condition IV incident, a limiting fault which is defined by the total rupture of a single stream generator tube. Due to the SGTR at full power operation, the primary coolant will be leaked to the secondary side and contaminate the secondary side with radioactive materials in the primary RCS coolant, such as fission products. [16] For this reason, SGTR could cause a severe accident, which may release radioactive materials, expressed as source terms, to the containment and later to the environment. [17]

Once the SG tube has ruptured and PRZ indicates the depressurization of the primary RCS, the charging pump automatically activates to maintain the RCS pressure level. Continuous depressurization of the primary RCS due to a loss of coolant through the ruptured SG tube will lead to a reactor and RCP trip followed by the MFW trip. The safety injection and AFW will be activated, resulting in an increasing RCS pressure and PRZ water level, and the RCS pressure trends toward the equilibrium value where the safety injection flow rate equals the flow through the ruptured SG tube.

For the secondary side, the turbine will trip as soon as the reactor is tripped, and excessive steam will be released to the steam dump. The high radiation level alarm will activate due to primary coolant leakage to the secondary side, and a monitor automatically isolates the secondary side systems and terminates discharge. The high radiation level alarm from the air ejector monitor automatically diverts the air ejector and the steam seal exhauster blower discharges through a filtration unit.

The major specific input settings for SGTR simulation are [9]:

- SGTR size is 2.4 cm^2 (0.002582 ft^2)

- Reactor trip at PRZ pressure drops below 13.3 MPa (1935.0 psia)

- RCP trips at T + 2 seconds from the reactor trip

- Initial steam flow loss is 514 kg/sec (1132.6 lbm/sec)

- AFW activation time was set to T + 30 seconds

- Low steam pressure safety injection signal of 5.5 MPa (800 psia)

3.4.2   Results and Discussion

Figure 24 shows nominal reactor power in the short and long-term during SGTR. The reactor power increased until the reactor trip (e.g., T + 42 seconds) and became a shutdown mode, which follows the decay heat power curve shown in Figure 4. No discrepancy was observed between 18 and 24 month burnup and Zr and FeCrAl cases. No Zion NPP FSAR data is available for comparison.
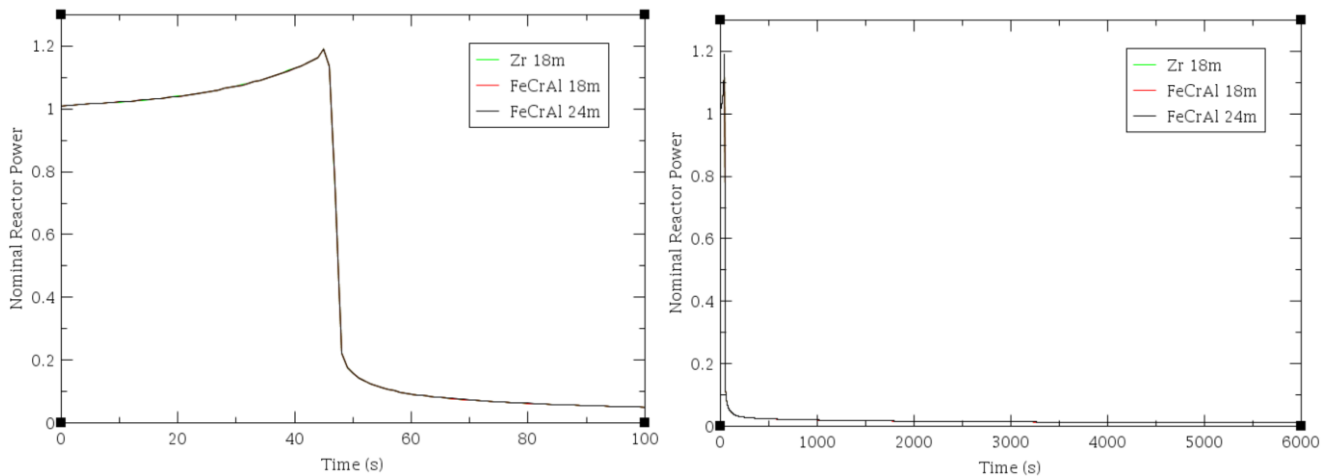
Figure 24. Nominal reactor power in short-term (left) and long-term (right) during SGTR.

Figure 25 shows RCS pressure and hot leg average temperature behavior during SGTR. The RCS pressure shows a similar trend compared to Zion NPP FSAR. [10] After a large depressurization near T + 3,800 seconds, the simulation result showed that the primary and secondary pressure became equal. The hot leg temperature behavior also shows a similar trend to the Zion NPP FSAR. [10] No discrepancy was observed between 18 and 24-month burnup and Zr and FeCrAl cases.
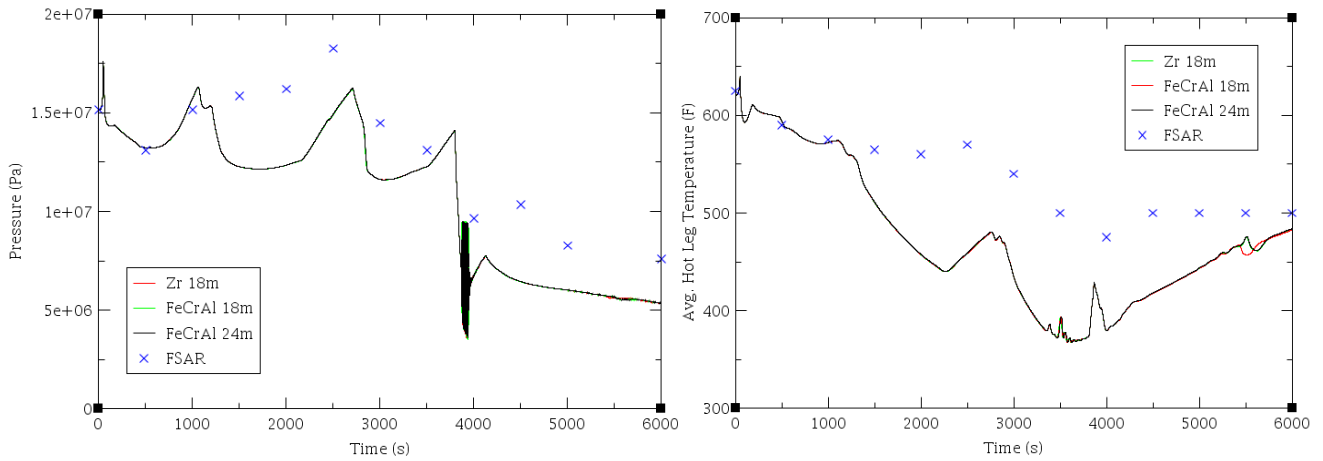
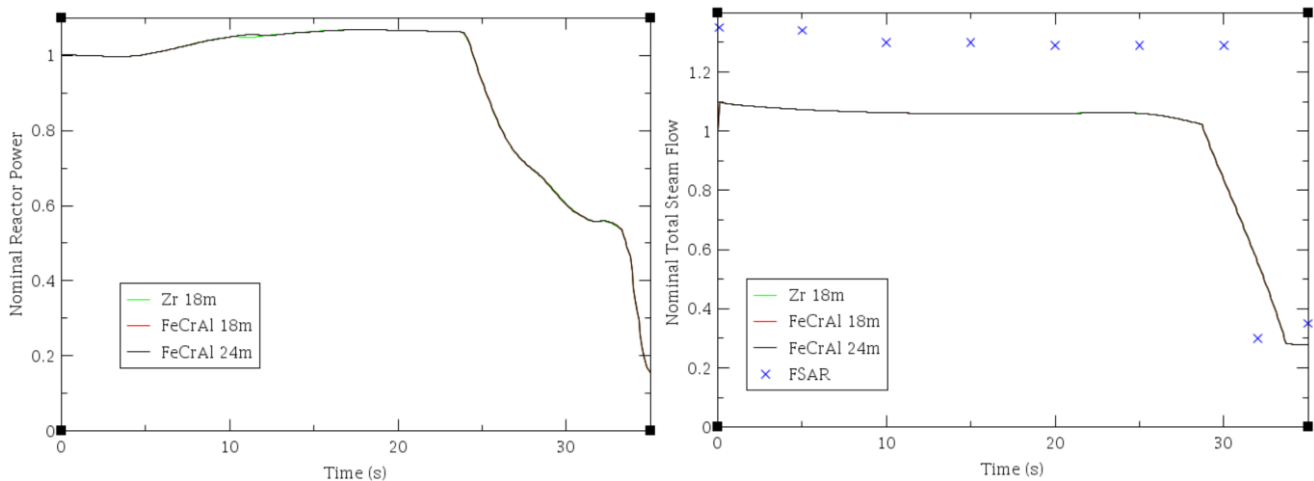Figure 25. PRZ pressure (left) and hot leg average temperature (right) during SGTR.

Figure 26 shows the short- and long-term PCT during SGTR. Both Zr and FeCrAl cladding showed a large temperature ramp when the reactor tripped (e.g., T + 42 seconds). Though no comparable FSAR data are available, based on the DNBR data in Figure 27, the coolant has exceeded the CHF value in this area. This could be due to coolant boiling; however, additional investigation is needed for this phenomenon. Fuel failure was not observed throughout the simulation of all cases.
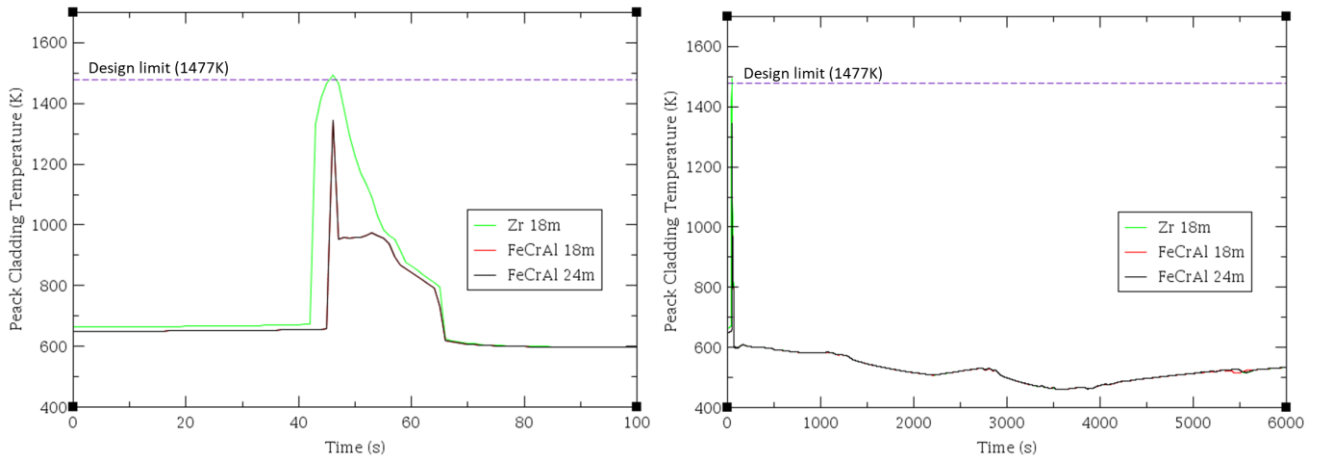
Figure 26. PCT during short-term (left) and long-term (right) during SGTR.
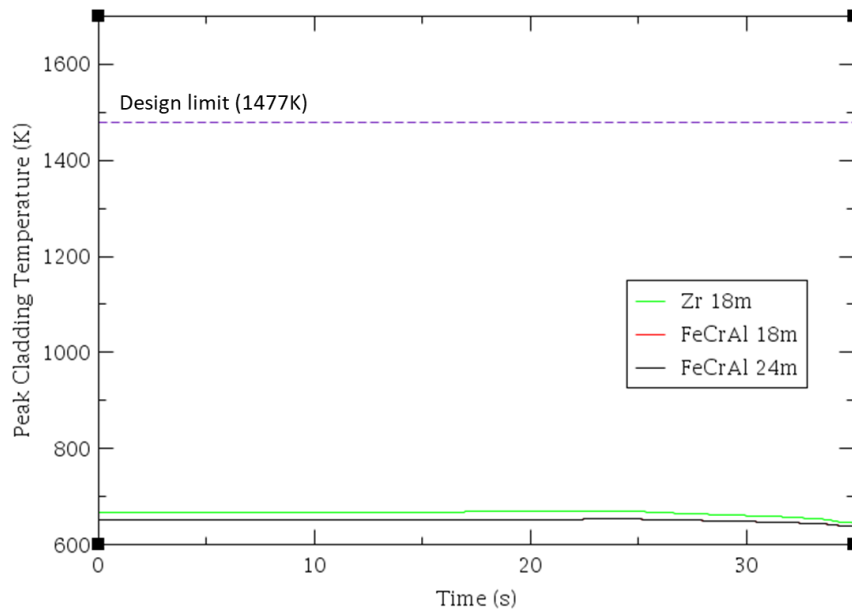
Figure 27 shows the amount of generated hydrogen and oxidation rate during SGTR. The value from FeCrAl cladding is negligible compared to those of Zr cladding.

36
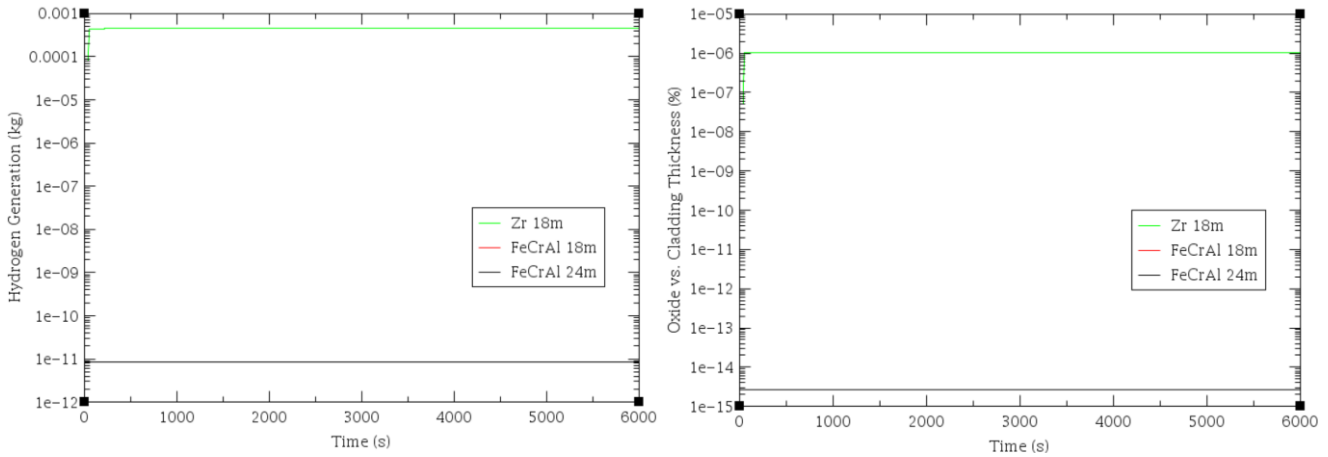
Figure 27. Hydrogen generation amount (left) and oxide vs. cladding thickness (right) during SGTR.

Figure 28 shows DNBR values during SGTR, which are comparable to FSAR. [10] However, the DNBR value dropped to zero near the reactor trip and after T + 65 seconds.

A steep PCT ramp was observed in the SGTR simulation when the reactor tripped and DNBR dropped to zero.
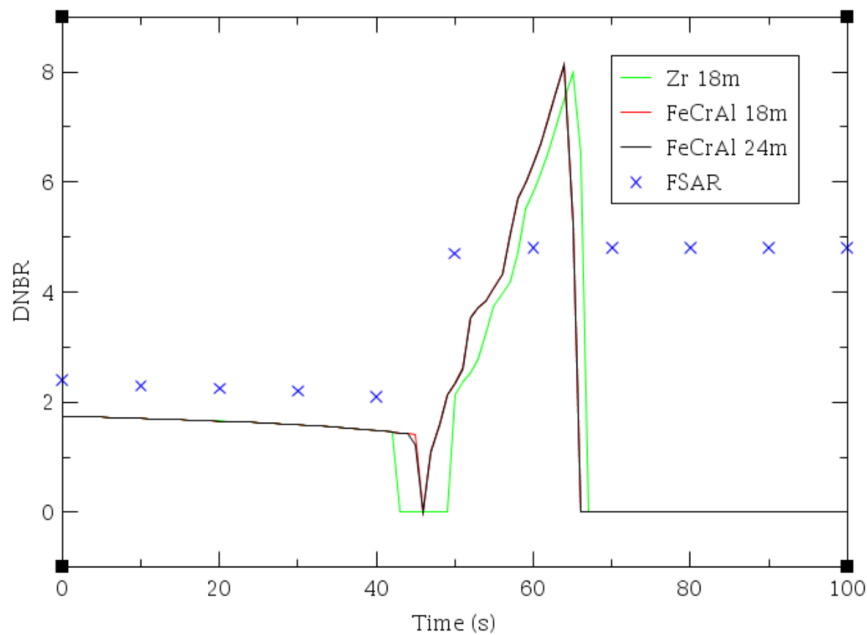
Figure 28. DNBR during SGTR. [10]

3.5 Condition IV Design-Basis Accidents: Large-Break Loss of Coolant Accident

3.5.1 Problem Description

LBLOCA is considered a limiting fault, an ANS Condition IV event, in that it is not expected to occur during the lifetime of the plant but is postulated as a conservative design-basis.

The LBLOCA is defined as a pipe rupture of the primary RCS with a total cross-sectional break area equal to or greater than 0.0929 m^2 (1.0 ft^2)[6]. [5][6] A double-ended guillotine break of the cold leg of the primary RCP was used in this analysis. Once a double-ended guillotine break occurred, the reactor coolant immediately flushed out to the containment as superheated steam.

As shown in Figure 29, this blowdown phase occurs just after the initial break and lasts approximately T + 30 seconds until ECCS is activated. From the normal operation coolant condition of 350°C with 15.5 MPa, the system pressure decreases very rapidly, causing primary coolant to flash out and a two-phase superheated steam near the break. Cladding temperature increases during the blowdown from normal operating conditions (325°C) to approximately 550–800°C (~1000–1500°F). In this phase, fuel temperature may fluctuate due to the reverse flow in the coolant loop and cool down the cladding temperature around T + 10 seconds. Near T + 20 seconds, the cladding temperature will rise again from the decay heat of nuclear fuel. In this sequence, fuel could be damaged by the plastic deformation of the cladding, mainly from the pressure difference across the fuel cladding. If the fuel peaking factor has a high rating (e.g., F_Q = 2.5), the cladding could even be deformed in the reflooding stage. The refill phase lasts about 10 seconds until the ECCS coolant completely refills the RPV lower plenum. The cladding temperature generally increases during this phase since decay heat removal is still sufficient. Once the water level in the lower plenum reaches the bottom of the active fuel, the reactor core starts to reflood. Reflooding from below allows a rapid cooldown (i.e., quenching) of the overheated fuel rods near T + 120~150 seconds. In this region, boiling could occur, and a high CHF will be shown. In some PWR designs, reflooding is possible from both the bottom and top of the core. The PCT will then decrease to the ECCS coolant temperature when the reflood phase ends about T + 250 seconds as an entire core is permanently filled with ECCS coolant. [18]
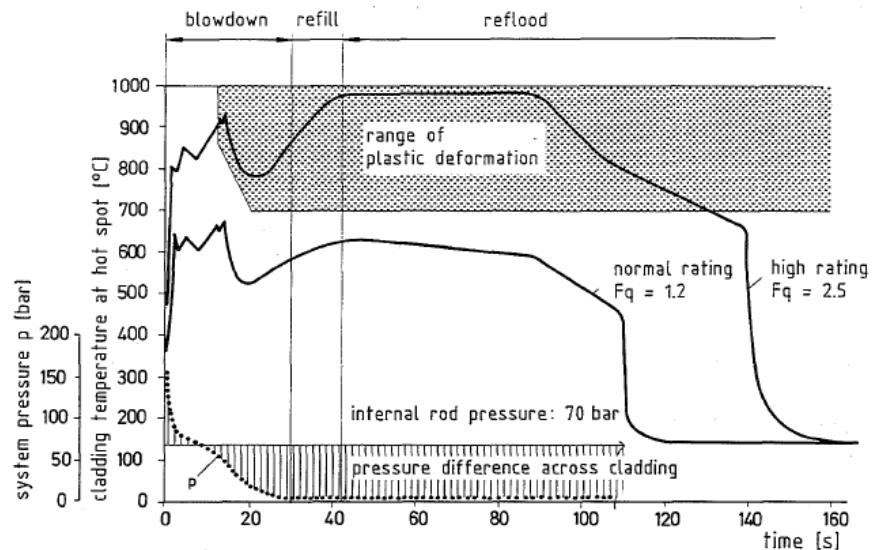
Figure 29. PCT and system pressure behavior during a double-ended cold leg break LBLOCA of a typical PWR. [18]

The major specific input settings for LBLOCA simulation are [9]:

- Break size set to 0.38 m^2 (4.1247 ft^2)

- Reactor trip at PRZ pressure drops below 13.0 MPa (1884.7 psia)

- RCP trip T + 0.1 second from reactor trip

---

[6] Break size equal to or larger than 0.0929 m^2 is categorized as an LBLOCA.

- Safety injection delay time was set to T + 40 seconds

- The accumulator activates when PRZ pressure drops below 4.2147 MPa (611.3 psia)

- Low steam pressure safety injection signal 5.5 MPa (100 psia)

3.5.2   Results and Discussion

Figure 30 shows the nominal reactor power and reactor coolant level. Compared to FSAR data, the nominal power decreases slower in the simulation result. The level of reactor coolant showed the core is uncovered during the accident. Compared to FSAR data, the core coolant level was lower which represents reflooding level is lesser than Zion NPP FSAR. [10] A peak was shown near T + 90 seconds for both nominal power and reactor coolant level. The main reasons are that the reactor pressure level dropped near ambient pressure (e.g., 0.1 MPa) and the boiling of the coolant occurred due to a quenching of the fuel as the reflood phase ends. The nominal power steeply increased from superheated steam generated by boiling but rapidly dropped as the refill and reflood continued.

No large discrepancy was observed between 18 and 24-month burnup and Zr and FeCrAl cases.
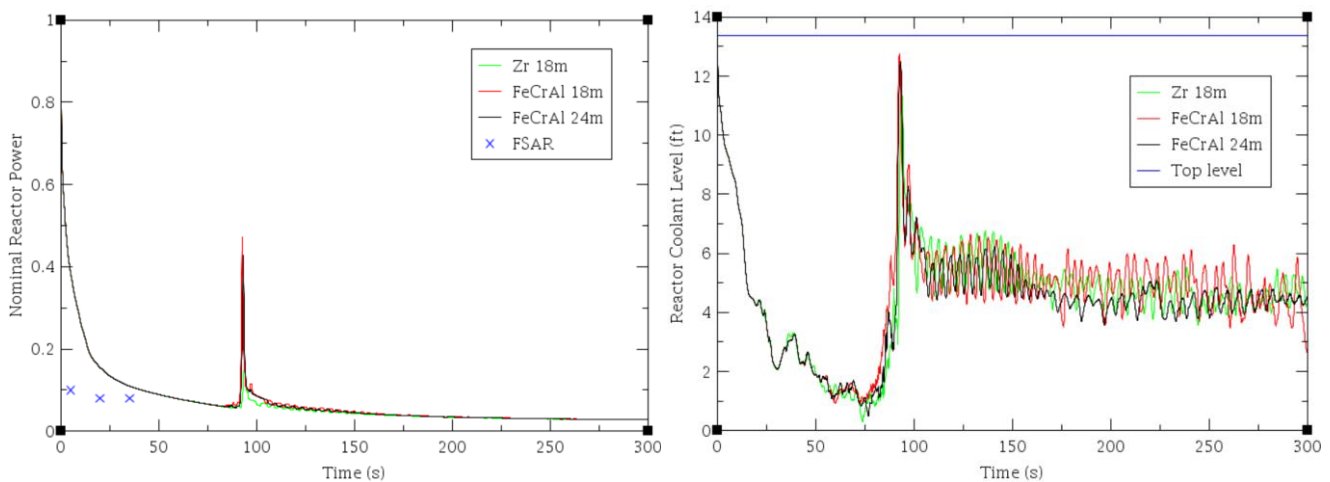
Figure 30. Nominal reactor power (left) and reactor coolant level (right) during LBLOCA.

Figure 31 shows the PRZ pressure and average hot leg temperature. Similar to the nominal reactor power in Figure 30, the PZR depressurizes immediately as flow loss through the break until. The pressure reached ambient (e.g., 0.1MPa) near T + 60 seconds, which eased boiling. The pressure reached a quasi-steady-state after T + 150 seconds but showed slower depressurization compared to the Zion NPP FSAR data. [10] This was because the current RELAP5-3D model does not correctly simulate reactor downcomer backflow during the LBLOCA blowdown phase, which needs accurate backward flow modeling. Further investigation is needed.

For the average hot leg temperature, FeCrAl with the 24-month burnup case shows slightly higher than other cases due to the larger amount of decay heat in higher burnup fuel.
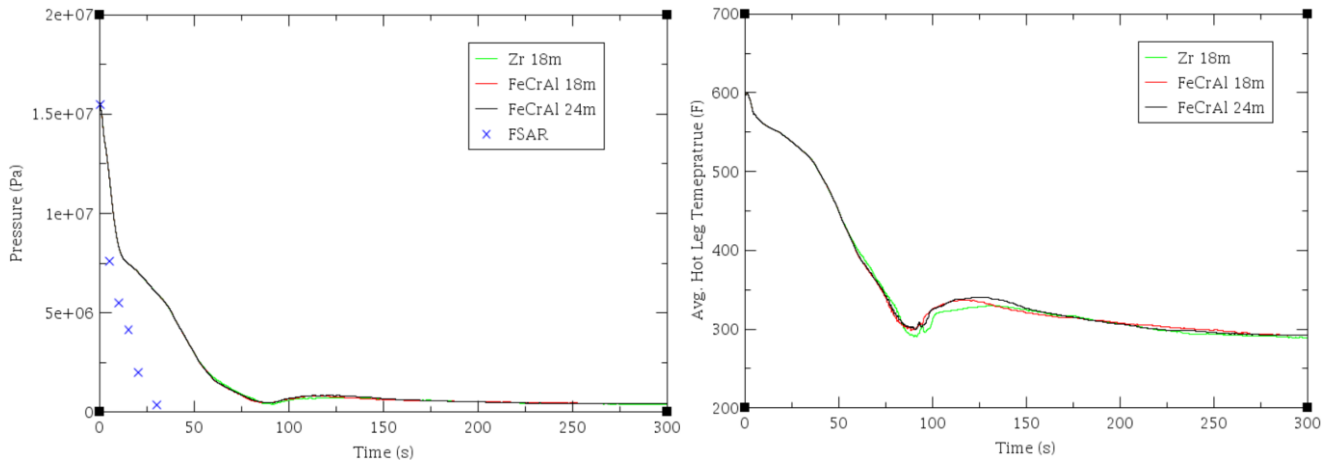
Figure 31. PRZ pressure (left) and hot leg average temperature (right) during LBLOCA.

Figure 32 shows PCT during LBLOCA. Compared to Zion NPP FSAR data, the temperature was lower for all cases. [10] The sequence of cooling is very similar to Figure 29, where the blowdown phase ends near T + 30 seconds. A rapid heat-up was shown during the refill phase from T + 30 to T + 40 seconds. A gradual heat-up was shown during the reflood phase from T + 40 seconds. A quenching occurred around T + 90 seconds as the reflood phase continued. PCT after the reflood (e.g., from T + 120) value was of FeCrAl with 24 months case shown higher than that of FeCrAl with 18 months since lower decay heat level in 18 months case. Zr with the 18-month burnup case showed the highest temperature behavior because it has more oxidation, which increases the local heat flux due to decreased heat transfer rate through a thicker oxidation layer (see Figure 33).

Though PCT did not reach the design limitation, fuel failure was observed for entire cases at the mid-high level (e.g., Node 4 and 5 of a total of six) of the hot fuel rod area. Table 6 shows fuel failure data from RELAP5-3D. Since the main driver of the fuel failure is the pressure difference between the inside and outside of the fuel rod, most fuel failures occurred when the RCS pressure reached ambient (e.g., 0.1 MPa) from T + 60 seconds. It is noted that the fuel failure result could be highly conservative, hence, further research is recommended by using a detailed fuel failure mechanism study.

Table 6. Fuel failure data.

Cladding Type	Node Number	Rupture Time (sec)	Flow Area Blockage Rate (%)
Zr 18 month	#4	63.835	61.866
Zr 18 month	#5	68.814	71.2
FeCrAl 18 month	#4	64.852	58.489
FeCrAl 18 month	#5	67.261	57.9
FeCrAl 24 month	#4	65.059	55.556
FeCrAl 24 month	#5	67.665	64.1
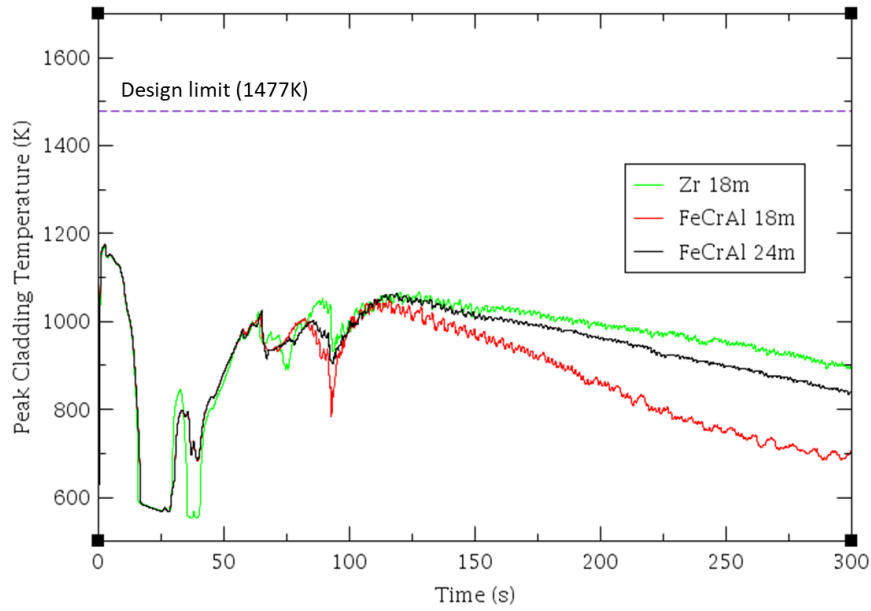
Figure 32. PCT during LBLOCA.

Figure 33 shows the amount of generated hydrogen and oxidation rate during LBLOCA. The value from the FeCrAl cladding is negligible compared to those of Zr cladding. A total of 0.01 kg of hydrogen was generated from Zr cladding while only 3~5E-6 kg of hydrogen was generated from both FeCrAl 18 and 24-month cases.
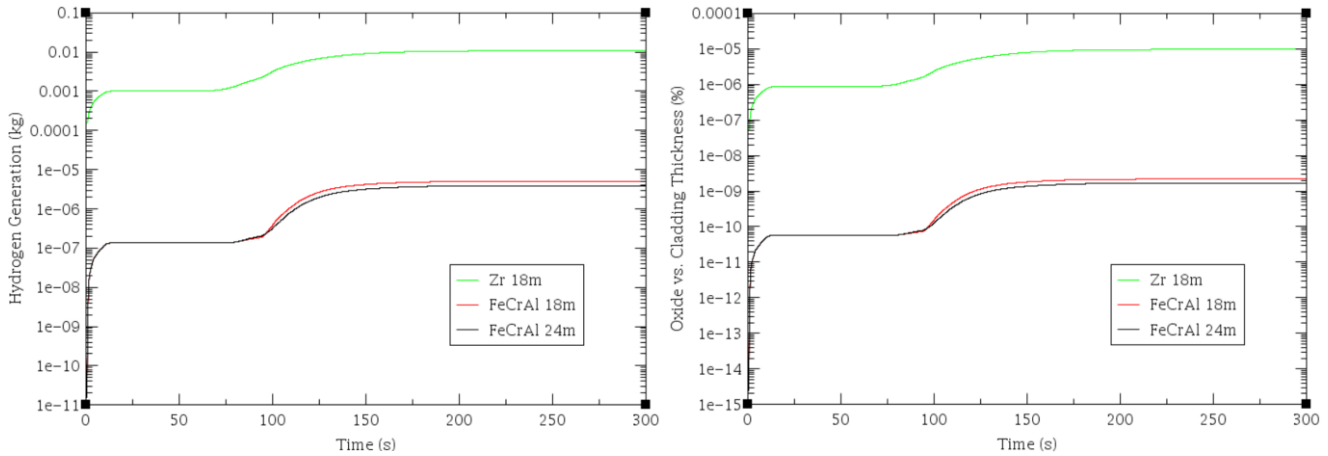
Figure 33. Hydrogen generation amount (left) and oxide vs. cladding thickness (right) during LBLOCA.

The DNBR during the LBLOCA in Figure 34 shows good agreement between RELAP5-3D and Zion NPP FSAR data. [10] The DNBR value of the Zr cladding dropped below the design limit (i.e., 1.2) at the beginning of the LBLOCA near T + 0.9 seconds.
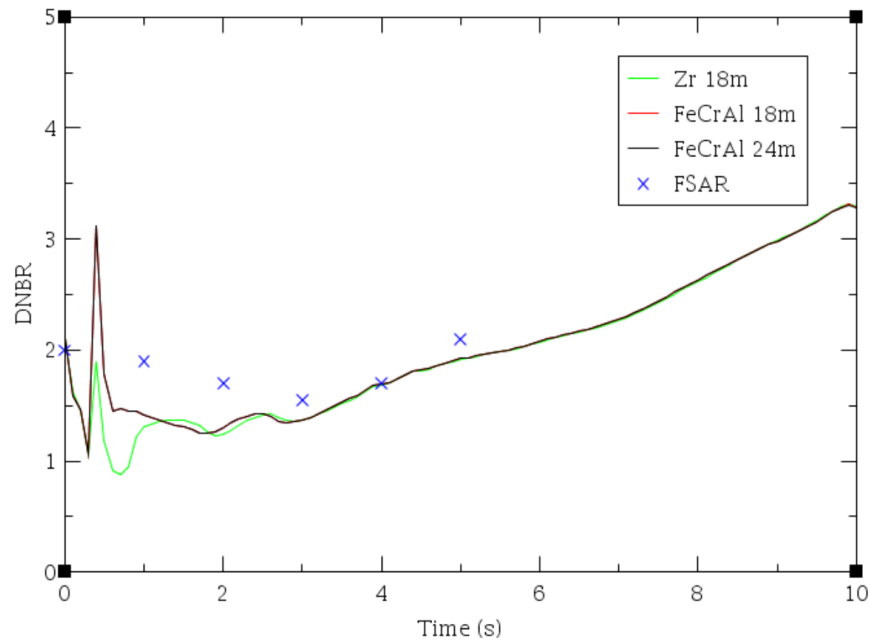
Figure 34. DNBR during LBLOCA. [10]

The RELAP5-3D model for the LBLOCA simulation showed a modeling issue in downcomer backward flow, and a slower depressurization made the late activation of ECCS and accident scenario similar to the recovered LBLOCA. A model upgrade is necessary to acquire more precise results. Despite modeling issues, results were generally comparable with FSAR data and the generic LBLOCA sequence. Both Zr and FeCrAl cladding failed at a similar time from the initial transient when the RCS pressure dropped to ambient pressure. Zr cladding generated notable amounts of hydrogen compared to FeCrAl cladding.

4. ANALYSIS ON THE BEYOND DESIGN-BASIS ACCIDENT

An analysis was performed for a severe accident analysis that was initiated from a recovered LBLOCA focusing on the source term and environmental consequences by using MELCOR and MACCS (MELCOR Accident Consequence Code System). [1] This recovered LBLOCA scenario has intentional delay of the LPSI activation time to damage core for source term analysis which was used as standard test problem of NRC (e.g., SOARCA report). [7] MELCOR/MACCS is a fully integrated, engineering-level severe accident consequence code developed to analyze the offsite consequences of a hypothetical release of radioactive material to the environment. The code models atmospheric transport and deposition; exposure as a result of inhalation, ingestion, and external irradiation; and emergency response and long-term remediation in a probabilistic approach. The uncertainties of source term were evaluated by the INL-developed stochastic code RAVEN (Risk Analysis Virtual ENvironment). [19]

The analysis includes both 18 and 24-month fuel cycles for Zr clad fuel and two different ATFs: FeCrAl APMT and FeCrAl C26M. The fission product inventory was calculated from the SCALE core lattice modeling code and VERA-CS high-fidelity depletion calculation tool. [1] The fission product inventory and decay heat data were developed for a 24-month cycle. An automatized tool was developed using the Python script to convert fission product inventory and decay heat data from the SCALE code to the class-wise MACCS format. The maximum distance was 1,000 miles from the plant with the accident to calculate the health, dose, and economic impacts.

The source term consequence analysis has more meaning in a relative sense. In the previous study, the amount of major source terms was less in an accident in a PWR with FeCrAl clad fuel compared to Zr clad fuel during both the 18 and 24-month cycles. [1] From this result, it is expected that the environmental impact will be lower when using ATF. However, this low environmental impact of ATF is not an authoritative indication of the source term decrease; instead, the fission product inventory is much higher in the higher burnup fuel cycle. The relative impact of an increased burnup and cladding material change will be different in other severe accident scenarios. During a severe accident initiated by a LBLOCA, the accident consequences may be very similar between lower and higher burnup cases, but higher burnup fuel will produce a larger fission product inventory. However, the released source term amount from ATF was found to be lower than Zr clad fuel since ATF shows smaller damage rate compared to Zr clad fuel. [1]

The uncertainty in source terms was analyzed by propagating the uncertainties in the FeCrAl material properties, which are mostly related to cladding properties (e.g., oxidation, cladding deformation, and fuel failure). The uncertainty propagation was set within the 95% tolerance limit (e.g., 95th percentile and 95% confidence) for the upper and lower boundary values. [20]

4.1 Model Description

4.1.1 Reactor Design

Figure 35 shows a diagram of the Westinghouse four-loop PWR Watts Bar NPP (WBN-1) Cycle 1 full-core layout on the left with an axial layout (which is publicly available data) of the fuel assembly on the right, which has similar power configuration with Zion NPP and used as the base of the reactor core design in MELCOR and MACCS analyses [1]. This core is filled with 193 fuel assemblies and has a rated thermal power of 3,411 MW. The main operating parameters of this core are shown in Table 7.
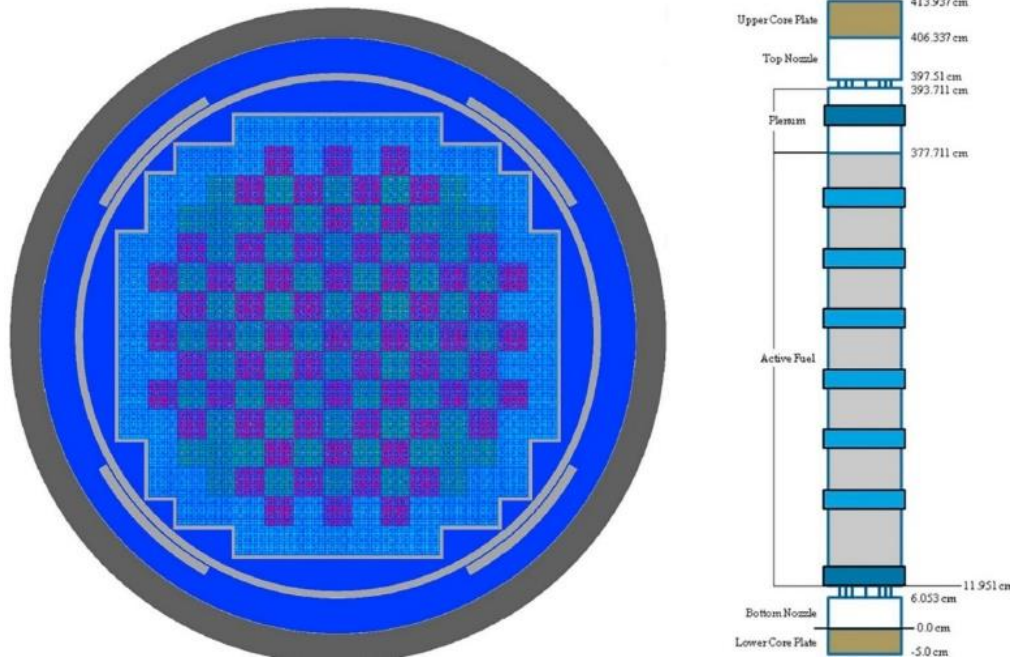
Figure 35. WBN-1 core diagram.

Table 7. Core characteristics for the generic PWR.

Parameter	Value
Rather thermal power (MWth)	3,411
Rated flow (kg/s)	18,231
Inlet temperature (K)	565
Coolant average temperature (K)	585
System pressure (MPa)	15.51
Coolant core bypass flow rate (%)	9.0

The fuel assembly used in this analysis consists of a 17 × 17 lattice of fuel rods. It is 21.50 cm wide and 406.337 cm tall, containing 264 fuel rods in an orthogonal array with six intermediate spacer grids and two end grids. The assembly also contains 24 guide tubes. Table 8 lists the fuel assembly geometry specifications with the nominal cladding thickness of 0.0572 cm. The FeCrAl fuel assembly was designed with a slight increase of 4.5 wt% for Zr clad fuel and 5.5 wt% for FeCrAl clad fuel. [1]

Table 8. Fuel geometry specifications.

Specification	Value
Fuel density (g/cc)	10.257
Assembly pitch (cm)	21.50
Rod pitch (cm)	1.26
Fuel pin radius (cm)	0.4096

Specification	Value
Inner cladding radius (cm)	0.4178
Outer cladding radius (cm)	0.4750
Inner guide tube radius (cm)	0.5610
Outer guide tube radius (cm)	0.6020
Enrichment (wt%)	4.5 (Zr clad) / 5.5 (FeCrAl clad)

The UO_2 fuel pins have an active stack height of 356.76 cm with a 152.4 cm height of solid axial blankets with 2.61 wt% enrichment at the top and bottom of the active fuel length. The reactor core is loaded with 84 fresh assemblies in a three-region, two-batch cycling scheme. These batches contain different numbers of integrated fuel burnable poison and wet annular burnable absorber (WABA) coated fuel rods, which is consistent with WBN-1. The WABA position is not constrained, and future effort is needed to set the correct WABA rod positions for the FeCrAl clad fuel assemblies.

Table 9 summarizes the main core design parameters and their limits. F_Q was to 2.1 for a more conservative result which used to be set as 2.5 based on the LBLOCA analysis. [1] $F_{\Delta H}$ represents the rod-integrated power thermal limit, which sets a limit on the fuel cladding CHF to ensure the departure from nucleate boiling does not occur. In this research, $F_{\Delta H}$ was 1.65, which is based on the previous safety evaluation of WBN-1. The rod-average discharge burnup limit was 62 GWD/MTU based on the current regulatory limit for the 18-month cycle. However, for the 24-month cycle that requires an extended burnup, the limit can be increased up to 75 or 80 GWD/MTU.

Table 9. Core design parameter limits.

Parameter	Limit
Heat flux hot channel factor (F_Q)	2.1
Enthalpy rise hot channel factor ($F_{\Delta H}$)	1.65
Peak pin burnup (GWD/MTU)	62
Peak boron concentration (ppm)	1,300
Moderator temperature coefficient (pcm/K)	0.0

4.1.2 Modeling of Beyond Design-Basis Accident Scenario

The WBN-1 reactor core model was applied to the MELCOR Zion NPP model was defined in the original NRC's severe accident analysis model [7]. The model was revised for the source term analysis which includes recovered LBLOCA scenario. Input detail is not publicly available.
Figure 36 shows the nodailization scheme for MELCOR modeling.
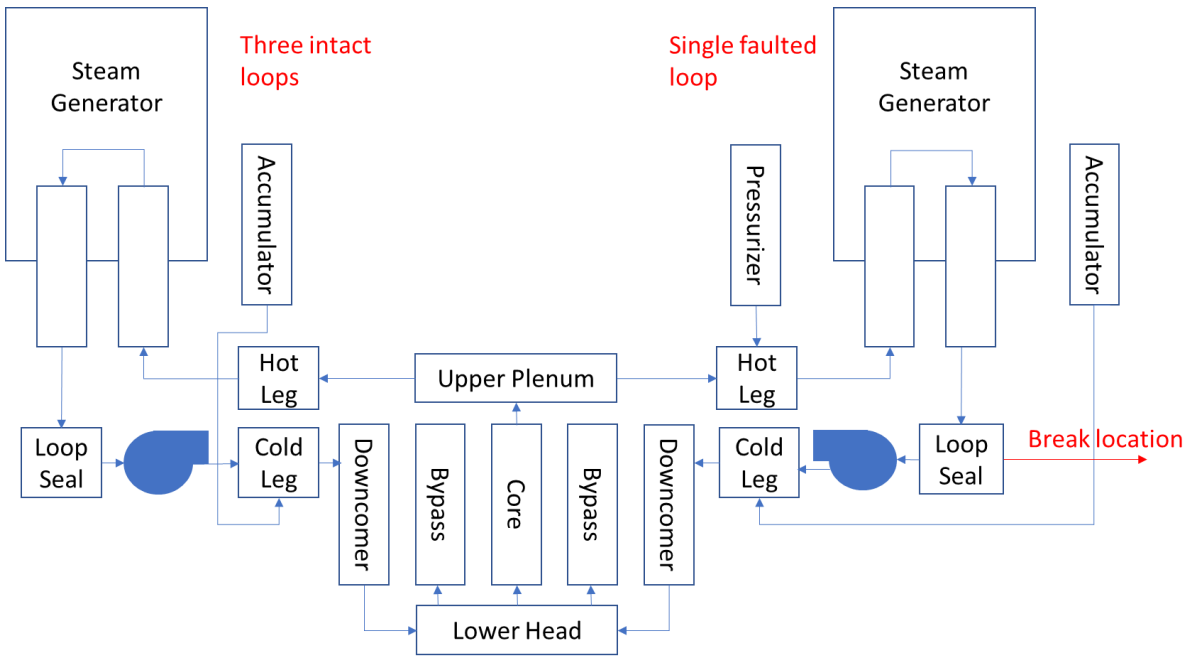
Figure 36. Nodalization for MELCOR modeling.

The accident time sequential is given in Table 10. The accident scenario assumed that the ECCS initially failed and that the LPSI system was reactivated at 27 minutes (1,620 seconds). The simulation will end at T + 6 hours (21,600 seconds). The accident time sequential was the same for both the 18 and 24-month cycle and Zr- and FeCrAl clad fuel models.

Table 10. Time sequential of the MELCOR LBLOCA scenario.

Event	Time (s)
Simulation starts	T − 200
Double-ended rupture in PRZ loop	T + 0
Reactor SCRAM	T + 0
Accumulator activation	T + 40 (at 4.275 MPa)
LPSI reactivation	T + 1,620
LPSI ends	T + 2,004
Simulation end	T + 21,600

4.1.3 Fission Product Inventory and Decay Heat

Based on the existing core design data from the VERA-CS depletion calculation [1], the fission product inventory and decay heat at the end-of-equilibrium core were calculated by SCALE core designing tool. Figure 37 shows a quarter of a 17×17 fuel assembly from SCALE lattice modeling with fuel pins (red), coolant (blue), and cladding.
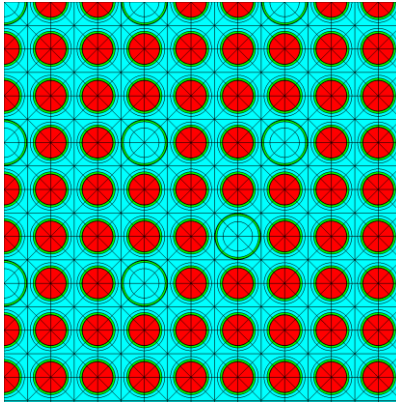
Figure 37. SCALE lattice model of quarter of a 17 × 17 fuel assembly.

Table 11 shows the fuel cycle performance parameters of the end-of-equilibrium core. For the demonstration, we used the core-averaged burnup value to generate the fission product inventory and decay heat data for MELCOR instead of pin-by-pin burnup data. For FeCrAl clad fuel, the average burnup and enrichment values are identical for both the APMT and C26M cases.

Table 11. Equilibrium cycle parameters of the 18 and 24-month fuel core.

Parameters	18 months, Zr clad	18 months, FeCrAl clad	24 months, FeCrAl clad
Core-averaged burnup (GWD/MTU)	33.2	33.2	45.1
Enrichment (wt%)	4.39	5.56	7.41

The decay heat is a function of time following the reactor scram. The decay heat is mostly generated from the short-lived isotope inventory and ^{239}Pu to ^{235}U fission based on the burnup rate. Figure 38 shows the decay heat curve generated from SCALE and used in MELCOR and MACCS simulations. No large difference was observed between 18 and 24 month burnup cycles.
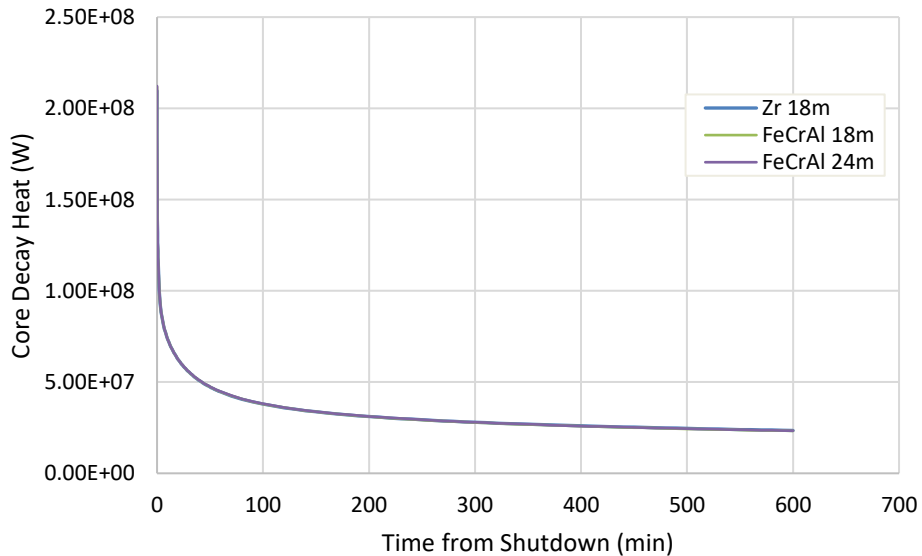
Figure 38. Decay heat is calculated by SCALE for each core.

Table 12 shows the radionuclide inventories for actinides and fission product isotopes calculated from SCALE, which are at least 0.01 kg/MTU. These data were used in MELCOR and MACCS simulations.

Table 12. End-of-equilibrium cycle inventories (Elements with at least 0.01 kg/MTU)

Element	Inventory at End-of-Equilibrium Cycle (kg/MTU)		
	Zr Clad 18 Months	FeCrAl Clad 18 Months	FeCrAl Clad 24 Months
Ag	0.06	0.05	0.07
Am	0.09	0.07	0.11
Ba	1.43	1.44	1.99
Br	0.02	0.02	0.03
Cd	0.07	0.06	0.08
Ce	2.84	2.89	3.78
Cs	2.92	3.02	4.20
Eu	0.14	0.13	0.18
Gd	0.07	0.06	0.09
I	0.20	0.19	0.25
Kr	0.39	0.40	0.55
La	1.25	1.26	1.72
Mo	3.29	3.32	4.57
Nb	0.04	0.05	0.05
Nd	3.71	3.76	5.26
Np	0.51	0.52	0.76
Pd	0.99	0.86	1.20
Pm	0.22	0.23	0.27
Pr	1.10	1.12	1.54
Pu	9.75	9.72	11.70
Rb	0.37	0.39	0.53
Rh	0.44	0.44	0.57
Ru	2.33	2.25	3.01
Sb	0.02	0.02	0.02
Se	0.06	0.06	0.08
Sm	0.63	0.63	0.88
Sn	0.06	0.05	0.07
Sr	0.98	1.04	1.40
Tb	0.00	0.00	0.00
Tc	0.83	0.84	1.12
Te	0.48	0.47	0.63
U	955.09	955.00	940.26
Xe	5.29	5.19	6.90
Y	0.51	0.53	0.73
Zr	3.73	3.85	5.25

4.1.4　Data Conversion for Source Term Analysis

The fission product inventories and decay heat data generated from SCALE were converted to the MELCOR/MACCS input format. The "element" level data from SCALE were resorted to MELCOR/MACCS "header element" level data by using the specifically developed Python script.

Table 13 summarizes the MELCOR/MACCS radionuclide classification, with two groups, CsI (#16 Cesium iodine) and CsM (#17 Cesium molybate), newly added to capture the accurate volatile behavior of I, Cs, and Mo.

Table 13. MELCOR/MACCS radionuclide classification.

Number	Chemical Group	Header Element	Elements
1	Noble gases	XE	Xe, Kr, Rn, He, Ne, Ar, H, N
2	Alkali metals	CS	Cs, Rb, Li, Na, K, Fr, Cu
3	Alkaline earths	BA	Ba, Sr, Be, Mg, Ca, Ra, Es, Fm
4	Halogens	I_2	I, Br, F, Cl, At
5	Chalcogens	TE	Te, Se, S, O, Po
6	Platinoids	RU	Ru, Pd, Rh, Ni, Re, Os, Ir, Pt, Au
7	Transition metals	MO	Mo, Tc, Nb, Fe, Cr, Mn, V, Co, Ta, W
8	Tetravalents	CE	Ce, Zr, Th, Np, Ti, Hf, Pa, Pu, C
9	Trivalents	LA	La, Pm, Sm, Y, Pr, Nd, Al, Sc, Ac, Eu, Gd, Tb, Dy, Ho, Er, Tm, Yb, Lu, Am, Cm, Bk, Cf
10	Uranium	UO_2	U
11	More volatile main group metals	CD	Cd, Hg, Pb, Zn, As, Sb, Tl, Bi
12	Less volatile main group metals	AG	Sn, Ag, In, Ga, Ge
13	Boron	BO_2	B, Si, P
14	Water	H_2O	WT
15	Concrete	CON	CC
16	Cesium iodide	CsI	—
17	Cesium molybdate	CsM	—

The developed Python script also calculates the distribution of iodine, cesium, and molybdenum across the CS, MO, CSI, and CSM classes based on the references that defined fission product inventories and decay heat during severe accidents. [1]

4.1.4.1　CsI Class

For the CsI class, the total mass of iodine in the core was assumed to be cesium iodide. The corresponding mass of cesium required to make up the compound was calculated using the ratio defined in the SOARCA report

[7]. In the SOARCA analysis, the ratio between cesium and iodine is 0.51155 to 0.48845 in the CsI class. Figure 39 shows the reclassification of the CsI class. The cesium radionuclide mass calculated from the SCALE ORIGEN package is subtracted from the total cesium element mass and added to the CsI class. The total amount of iodine was added in the CsI class.
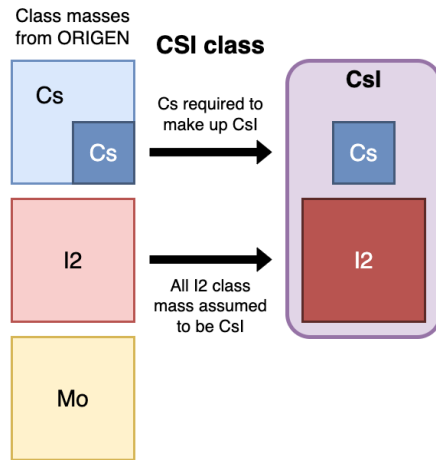
Figure 39. Reclassification of CsI class elements.

4.1.4.2   CS Class

The fission product released to the fuel cladding gap was 5% of the total cesium from the CsI class and pure cesium in the fuel [7]. Figure 40 shows the reclassification of CS class from CsI class and pure cesium. Since iodine in CsI class contains all the iodine present in the reactor, 5% of iodine from the CsI class will be present in the gap. In other words, 95% of iodine will be present in the CsI class while 5% will be in the gap in the CS class.
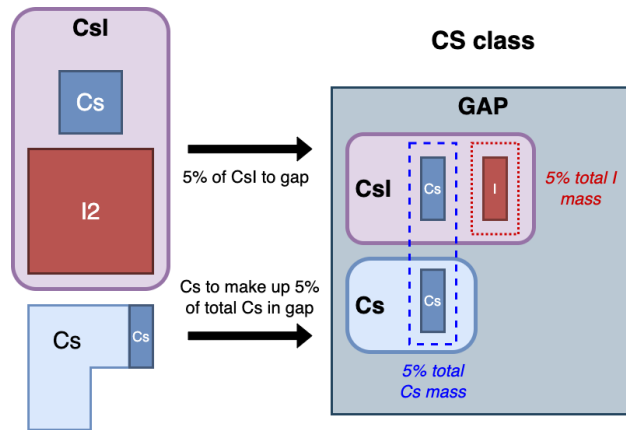
Figure 40. Reclassification of CS class.

4.1.4.3   CsMo and Mo Classes

As shown in Figure 41, the remaining cesium mass left after the CsI and CS class contributions was assumed to be in the CSM class. The ratio between cesium and molybdenum is 0.734789 to 0.265211 in the CSM class [7]. The molybdenum mass is subtracted from the total amount based on this ratio and is added to the CSM class. The remaining molybdenum mass is then allocated to the MO class, as shown in Figure 42.
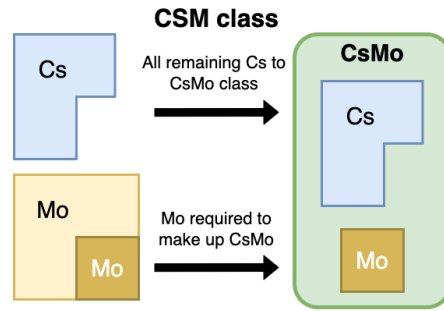
Figure 41. Reclassification of the CSM class.
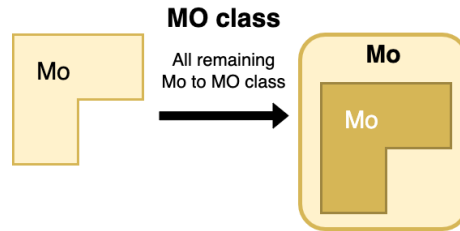
Figure 42. Reclassification of the MO class.

4.2   Uncertainty Quantification in Source Term Analysis

4.2.1   Problem Description

The uncertainty analysis of the C26M FeCrAl clad fuel with 18 months of burnup was performed based on the propagation to five parameters, mainly effects on the core damage, hydrogen generation, and source term analysis:

- Oxidation start temperature (K)

- Breakaway oxidation start temperature (K)

- Rod burst temperature (K)

- CsI group fraction in the fuel gap (%)

- Xe group fraction in the fuel (%).

The breakaway oxidation is a unique phenomenon of Zr alloys, which is one factor in unstable oxide growth. This phenomenon was observed during the LBLOCA analysis between 600°C and 1,050°C, with a rapid increase in oxidation rate and hydrogen generation. This phenomenon enhances the deterioration of mechanical cladding properties due to the embrittlement effect of oxides and hydrogen. Hence, it is an important parameter to maintain fuel and cladding integrity during transient accidents. [21]

Table 14 shows uncertainty boundaries for the above five parameters. A Gaussian distribution was used to sample each of the parameters, for which about 95% of the data is within 2 standard deviations (i.e., 2σ) from the mean value. [22] For the breakaway oxidation start temperature, the deviation was set based on the difference between the lowest reported value and FeCrAl melting temperature. The Monte Carlo randomization method was used for uncertainty propagation through RAVEN.

Table 14. Initial uncertainty boundaries for FeCrAl property-related parameters.

Parameter	Mean	Standard Deviation (σ)	Remark
Oxidation start temperature (K)	1,32	33	Lows oxidation rate was observed below about 1,473 K. [23] Small σ value was assumed as 2.5% of mean value (e.g., 33 K).

Parameter	Mean	Standard Deviation (σ)	Remark
Breakaway oxidation start temperature (K)	1,748	25	The breakaway oxidation temperature varies with Cr content and can be higher for FeCrAl APMT. σ of 25 K is the best estimate difference between the breakaway oxidation temperature. [24] Note that FeCrAl melts at 1,773K, so when the breakaway oxidation start temperature is higher than this (as is the case for APMT) then breakaway oxidation does not occur.
Rod burst temperature (K)	1,173	58.65	No experimental data is available. Large σ value was assumed as 5% of mean value (e.g., 58.65 K).
CsI group fraction	5.0	1.25	FFRD increases halogen and alkali metal dispersal by 2%. [25] Hence, 2% of σ value was used (e.g., 1.25 K).
Xe group fraction	5.0	1.25	FFRD increases halogen and alkali metal dispersal by 2%. [25] Hence, 2% of σ value was used (e.g., 1.25 K).

The order statistics approach was used to decide the minimum number of necessary calculations for the uncertainty propagation, which is based on Wilks' formula. [26] This method implies no assumptions on the probabilistic distribution function of the figure of merit and an unlimited number of model uncertainties can be considered at the same time during the sampling process. [27] Hence, the U.S. NRC requirement in 10 Code of Federal Regulation (CFR) 50.46 states that there must be a high level of probability that the regulatory limits are not being exceeded, which suggests a minimum of 59 calculations for the uncertainty propagation of 95% of the population with 95% confidence. In this research, 60 calculations were therefore conducted to meet the NRC's suggestion.

Table 15 shows the updated uncertainty boundaries of Table 14 after 60 calculations. Sample mean values were similar to those of the initial values in Table 14. Minimum and maximum values in the sample are also shown, which in all cases are around 2 standard deviations from the mean, suggesting adequate coverage of the sample space.

Table 15. Updated uncertainty boundaries after 60 calculations and the difference between initial values (% error).

Parameter	Mean (% error)	Standard Deviation (% error)	Minimum	Maximum
Oxidation start temperature (K)	1,322.78 (-0.01%)	36.72 (11.28%)	1,218	1,395
Breakaway oxidation start temperature (K)	1,767.66 (1.13%)	22.86 (-8.54%)	1,704	1,811
Rod burst temperature (K)	1,167.48 (-0.47%)	58.16 (-0.83%)	1,060	1,296
CsI group fraction in fuel gap	4.980 (-0.40%)	1.18 (-5.72%)	1.79	7.38
Xe group fraction in fuel	5.035 (0.69%)	1.54 (23.37%)	1.82	8.54

4.2.2   Results and Discussion

Figure 43, Figure 44, and Figure 45 show core damage, hydrogen generation, and total source term release of FeCrAl clad with an 18-month burnup cycle along with their uncertainties propagated from FeCrAl properties, respectively. The upper boundary of core damage in the FeCrAl case was higher than in the Zr cladding case. The hydrogen generation rate of the FeCrAl case upper boundary was similar to that of the Zr cladding case. The amount of source term from the Zr cladding case was almost two times higher than that of the FeCrAl case upper boundary values.
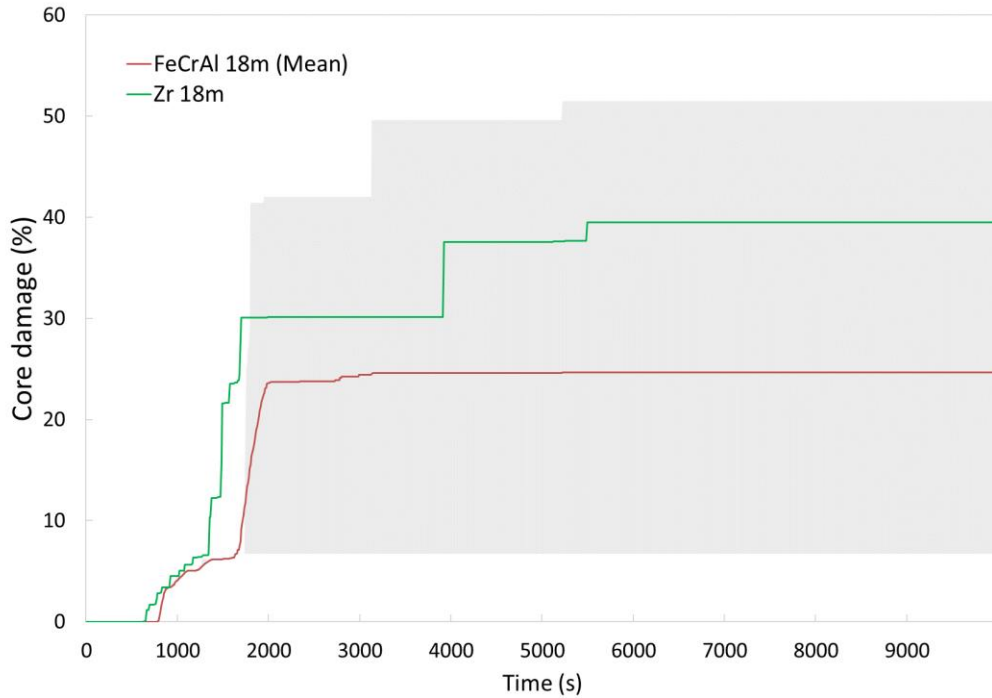
Figure 43. Uncertainties of FeCrAl 18m case in core damage.
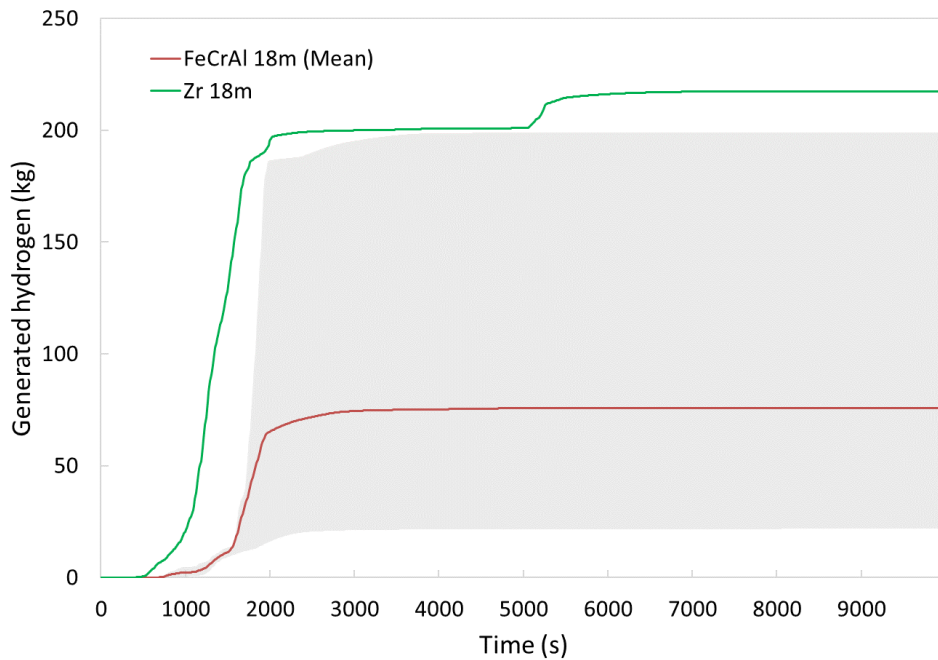
Figure 44. Uncertainties of FeCrAl 18m case in hydrogen generation.
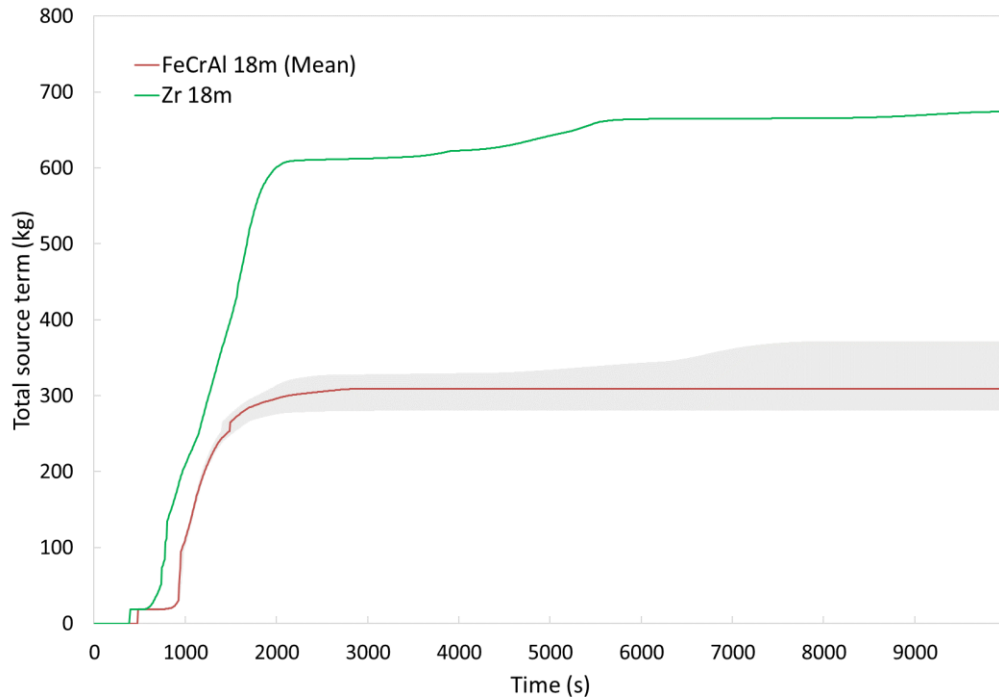
Figure 45. Uncertainties of FeCrAl 18m case in total source term release.

The mean value of hydrogen generation is found down-positioned near the lower uncertainty boundary values. To understand this phenomenon, this study used a covariance matrix approach, which can describe the correlation coefficient between two different random values (e.g., input and output values). [28] The correlation between two random values becomes stronger as the coefficient gets closer to ±1, and less correlation as the value approaches zero. Table 16 shows the correlation coefficient between propagated input parameters and output data. The coefficient of the breakaway oxidation start temperature and entire output data are closest to -1, which means a very strong correlation between breakaway oxidation start temperature and core damage, hydrogen generation, and total source term. In other words, breakaway oxidation start temperature is the most important parameter for the output data. As the breakaway oxidation start temperature increases and decreases the oxidation rate at a lower temperature, the fuel integrity will remain to reduce core damage, hydrogen generation, and less source term release. This strong correlation between breakaway oxidation start temperature and output leads to a bias of mean value, which is shifted down from the center.

Table 16. The correlation coefficient between input parameters and output results of the FeCrAl cladding case.

Parameter	Oxidation Start Temperature (K)	Breakaway Oxidation Start Temperature (K)	Rod Burst Temperature (K)	CsI Group Fraction	Xe Group Fraction
Core damage (%)	0.022	-0.79	0.28	0.0018	0.059
H_2 generated (kg)	0.10	-0.90	0.29	0.035	0.055
Total source term (kg)	-0.087	-0.62	0.058	0.14	0.38

4.3 Consequence Analysis of Environmental Impact

4.3.1 Problem Description

Most of the input parameters were set to default in MACCS including meteorology, site, dose coefficient, and food ingestion data. The fission product inventory and release source term data was provided from MELCOR simulation. The weather data from the Surry NPP was used with a sampling frequency of 1 hour,

which is also the default parameter in MACCS. For the plume modeling, the Latin hypercube sampling method was applied for the probabilistic assessment of the result.

MACCS divides isotopes into 10 groups based on particle size. Each particle size is handled differently by the atmospheric transport model. As part of converting MELCOR output files to MACCS inputs, MACCS estimates the composition of the plume based on the core inventory at the time of release and the released mass of each MELCOR chemical class.

Three results were reviewed for the consequence analysis: latent health effect (i.e., total cancer fatalities), population dose (i.e., total dose delivered), and economic consequence within the range of 10, 50, and 1,000 miles from the accident origin.

4.3.1.1   Latent Health Effect

MACCS simulates both early and latent (i.e., cancer risk) health effects. [29] Four stochastic health effects models are available for the latent health effect modeling in MACCS:

- Linear no-threshold model

- Linear quadratic model

- Piecewise-linear model

- Annual dose threshold model.

This study used the linear no-threshold model for the latent health effect. For the cancer risk, MACCS calculates risk from the exposure rate from each human organ and the total based on the Biological Effects of Ionizing Radiations (BEIR V) commission model [29]. The relevant input parameters were default.

4.3.1.2   Population Dose

MACCS uses a dose coefficient approach coupled with a set of dose-response models for early and late health effects. For external exposures, a dose coefficient is a factor that relates the radionuclide quantity in an environmental media outside of the body, such as soil or air, to the radiation dose received. For internal exposures, a dose coefficient is a factor that relates the quantity of a radionuclide that is ingested or inhaled to the radiation dose received. [29]

MELCOR calculates the dose coefficient for each radionuclide and organ through exposure types:

- Cloud-shine dose rate factor [$Sv/(Bq\text{-}s/m^3)$]

- Ground-shine dose rate factor [$Sv/(Bq\text{-}s/m^2)$]

- Acute, short-term inhalation doses (Sv/Bq) for calculating early, deterministic health effects

- Lifetime, 50-year committed inhalation doses (Sv/Bq) for calculating effective doses and late, stochastic health effects from inhalation

- Lifetime, 50-year committed ingestion doses (Sv/Bq) for calculating effective doses and late, stochastic health effects from food and water ingestion.

In this study, we calculated two long-term doses (i.e., two last dose coefficients from inhalation and ingestion). The relevant input parameters were set as default.

4.3.1.3   Economic Consequences

MACCS employs a cost-based evaluation of economic impacts to calculate the costs of intermediate and long-term phase relocation and interdiction from a severe accident, [29] including:

- Daily costs incurred during temporary evacuation and relocation

- One-time relocation costs from temporary or permanent interdiction

- Decontamination costs for property that can be returned to use

- Lost return on investment from temporarily interdicted properties

- Depreciation of temporarily interdicted properties

- The value of permanently interdicted property (i.e., condemned)

- Economic losses of milk and crops destroyed or not grown.

    The sum of the above losses is shown in this study. The relevant input parameters were default.

4.3.2   Result and Discussion

    We considered five cases for MELCOR/MACCS simulation:

- Zr clad, 18 month cycle

- FeCrAl clad (C26M), 18 month cycle

- FeCrAl clad (C26M), 24 month cycle

- FeCrAl clad (APMT), 18 month cycle

- FeCrAl clad (APMT), 24 month cycle.

    The difference between the two FeCrAl cladding case types, C26M and APMT, is mainly the cladding oxidation model. The result does not bind the quality of different cladding materials.

    The simulation results of cancer fatality, long-term dose, and total economics costs are in Table 17, Table 18, and Table 20, respectively, where "prob. non-zero" indicates whether the consequence will appear or not. For example, if a dose exposure was found, the "prob. non-zero" value will be always one, regardless of weather conditions. This implies the radiological impact is well simulated during the MACCS calculation. In the case of economics analysis, if the "prob. non-zero" value is less than one, there might be no need to decontaminate farmland or relocate large groups of people for a long time if the weather is good.

    In general, FeCrAl clad cases show less of an impact compared to the Zr clad case in either an 18 or 24 month cycle. The main reason is that the FeCrAl cladding mitigates the release of a major source term during defined LOCA scenarios.

    Table 17 shows total cancer fatalities between 10, 50, and 1,000 miles from the accident origination. The cancer risk was calculated from the lifetime dose, which is assumed to be 50 years from the time of initial exposure, including evacuated and non-evacuated cohort groups.

Table 17. Total cancer fatalities.

Cladding	Distance (mile)	Prob. Non-Zero	Mean	50th Percentile	Peak Consequence	Peak Probability
FeCrAl 24 month APMT	0–1,000	1	1.37	1.20	8.79	1.15E-3
	0–50	1	0.647	0.500	6.85	1.15E-3
	0–10	1	0.578	0.441	2.96	3.90E-4
FeCrAl 18 month APMT	0–1,000	1	0.760	0.664	4.77	1.15E-3
	0–50	1	0.372	0.262	3.71	1.15E-3
	0–10	1	0.335	0.231	1.88	3.90E-4
FeCrAl 24 month C26M	0–1,000	1	1.71	1.49	11.1	1.15E-3
	0–50	1	0.789	0.610	8.63	1.15E-3
	0–10	1	0.700	0.557	4.18	3.90E-4
	0–1,000	1	0.762	0.671	4.78	1.15E-3

FeCrAl 18 month C26M	0–50	1	0.371	0.274	3.72	1.15E-3
	0–10	1	0.333	0.248	1.78	1.14E-3
Zr 18 month	0–1,000	1	2.72	2.33	20.3	1.15E-3
	0–50	1	1.02	0.710	15.7	1.15E-3
	0–10	1	0.878	0.629	5.02	1.14E-3

The total long-term dose in Table 18 is the sum of dose from the population exposed between 1 week and 50 years after the accident.

Table 18. Total long-term dose (person-Sv).

Cladding	Distance (mile)	Prob. Non-Zero	Mean	50th Percentile	Peak Consequence	Peak Probability
FeCrAl 24 month APMT	0–1,000	1	24.6	20.8	153	1.15E-3
	0–50	1	9.28	7.40	116	1.15E-3
FeCrAl 18 month APMT	0–1,000	1	13.2	10.8	82.8	1.15E-3
	0–50	1	4.51	3.29	62.0	1.15E-3
FeCrAl 24 month C26M	0–1,000	1	31.2	25.7	193	1.15E-3
	0–50	1	11.6	9.10	147	1.15E-3
FeCrAl 18 month C26M	0–1,000	1	13.4	11.0	82.9	1.15E-3
	0–50	1	4.61	3.54	62.2	1.15E-3
Zr 18 month	0–1,000	1	51.7	40.7	352	1.15E-3
	0–50	1	14.0	9.86	263	1.15E-3

Table 19 shows a comparison of the peak 2-hour dose. The 10 CFR 50.67 sets a TEDE limit of 0.25 Sv in 2 hours for the individual located 10–13 miles from the accident location. [8] All data were less than the regulatory limit of 0.25 Sv. The peak dose was about 50% less in all FeCrAl clad cases compared to the Zr clad case, even in a peak consequence analysis. Increasing the cycle length from 18 to 24 months only increases the projected peak dose by around 10%.

Table 19. Peak 2-hour dose (Sv).

Cladding	Distance (miles)	Prob. Non-Zero	Mean	50th Percentile	Peak Consequence	Peak Probability
FeCrAl 24 month APMT	10–13	1	1.92E-4	1.28E-4	1.08E-3	1.15E-3
FeCrAl 18 month APMT	10–13	1	1.75E-4	1.18E-4	9.81E-4	1.15E-4
FeCrAl 24 month C26M	10–13	1	2.09E-4	1.42E-4	1.09E-3	1.14E-3

FeCrAl 18 month C26M	10–13	1	1.82E-4	1.27E-4	9.08E-4	1.14E-3
Zr 18 month	10–13	1	3.98E-4	2.62E-4	2.14E-3	1.14E-3

The economic cost in Table 20 is the sum of remediation cost up to 30-years after the accident. The cost values of Zr 18-month and FeCrAl 24 month cases are very similar.

Table 20. Total economic costs ($).

Cladding	Distance (mile)	Prob Non-Zero	Mean	50th percentile	Peak Consequence	Peak Probability
FeCrAl 24 month APMT	0–1,000	1	1.08E7	2.24E7	5.97E7	1.15E-3
FeCrAl 18 month APMT	0–1,000	1	7.59E6	6.32E6	3.75E7	1.15E-3
FeCrAl 24 month C26M	0–1,000	1	1.38E7	1.14E7	7.26E7	1.16E-3
FeCrAl 18 month C26M	0–1,000	1	8.70E6	7.65E6	2.57E7	2.00E-4
Zr 18 month	0–1,000	1	1.13E7	1.04E7	7.59E7	3.90E-4

4.3.3 Uncertainty Analysis in Consequence Analysis

Same as the MELCOR uncertainty analysis in Section 4.2, MACCS simulations were also conducted for 60 calculations to analyze uncertainties in a consequence analysis for the case of C26M FeCrAl clad fuel with 18 months burnup cycle compared with Zr clad fuel with 18 months case. The uncertainty perturbation was from FeCrAl material properties as shown in Table 14 and Table 15.

Figure 46 and Figure 47 show uncertainties in total cancer fatalities and peak 2-hour dose as distance increases from the accident location to 1,000 miles, respectively. Similar to the source term uncertainty analysis result in Section 4.2, the upper boundary of FeCrAl clad fuel was lower than the Zr clad case.
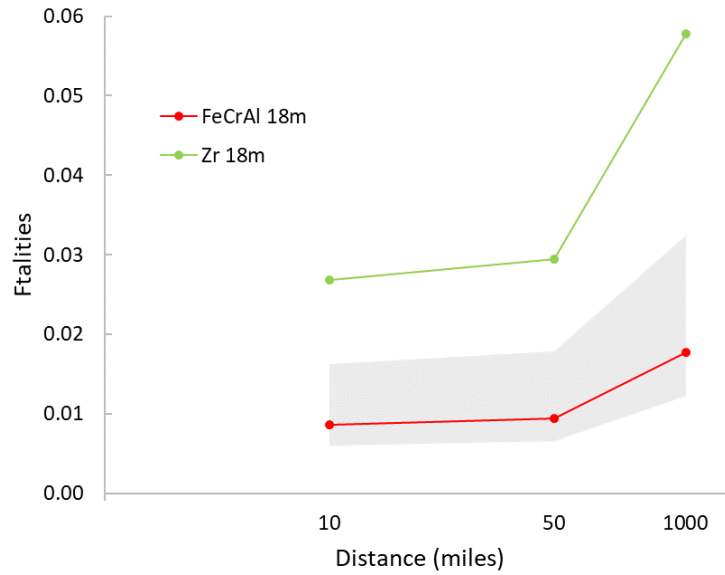
Figure 46. Uncertainties of FeCrAl 18m case in total cancer fatalities.
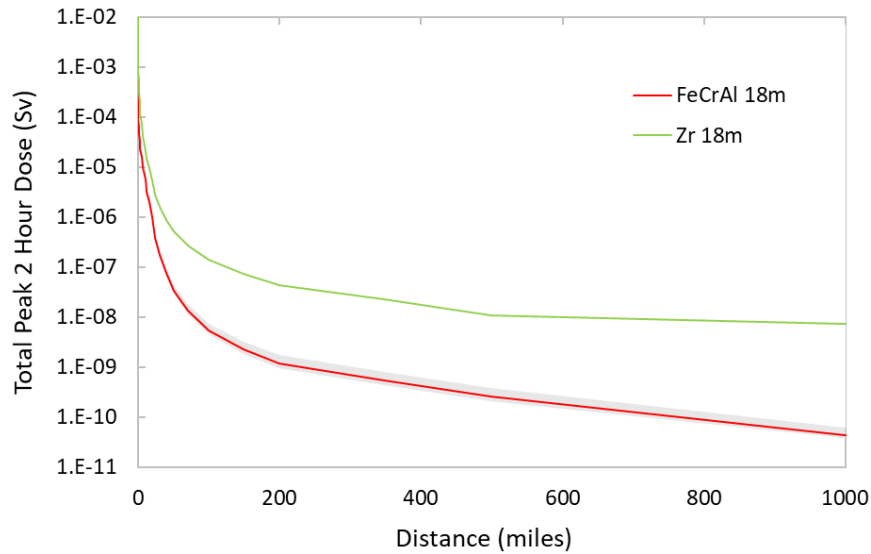
Figure 47. Uncertainties of FeCrAl 18m case in total peak 2 hour dose.

Figure 48 and Figure 49 show uncertainties in total cancer fatalities and total long-term dose within 1,000 miles from the accident location. Figure 50 shows the total peak 2-hour dose within 10 miles of the accident location. The uncertainties are given with the error bars. In all instances, FeCrAl resulted in less severe consequences than Zr clad fuel due to the lower release rate of the source term.
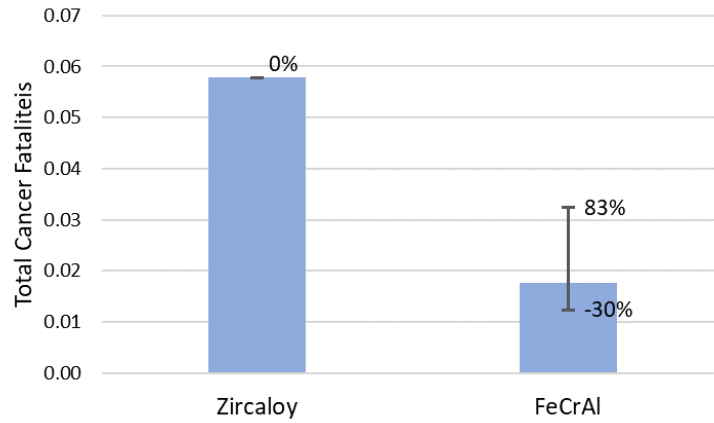
Figure 48. Uncertainties of FeCrAl 18m case in total fatalities within 1,000 miles of the accident.
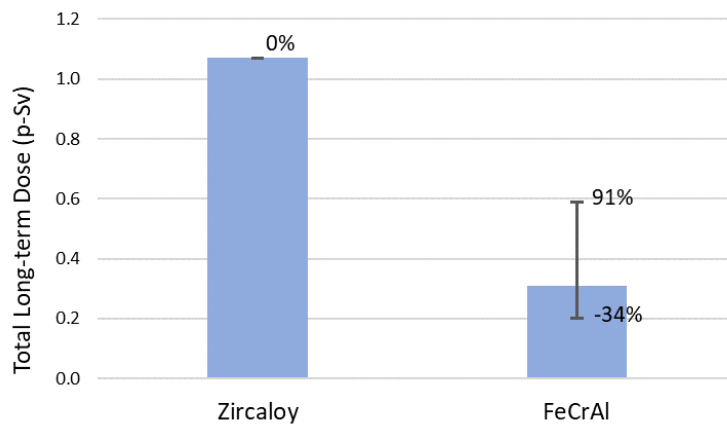
Figure 49. Uncertainties of FeCrAl 18m case in total long-term dose per person within 1,000 miles of the accident.
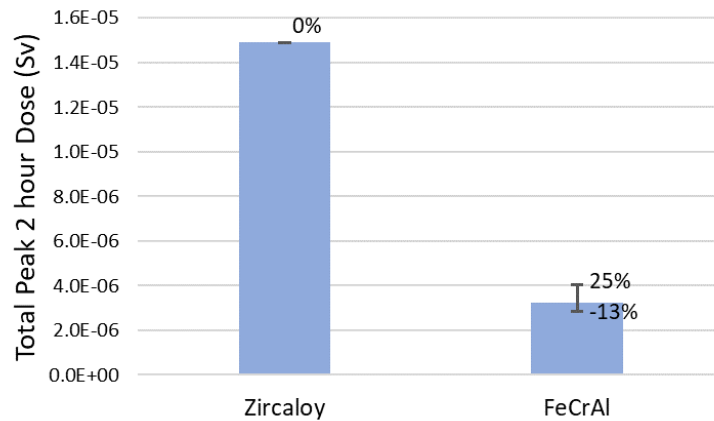
Figure 50. Uncertainties of FeCrAl 18m case in total peak 2 hour dose within 10 miles of the accident.

5.   CONCLUSIONS AND FUTURE WORK

Safety analyses of FeCrAl ATF clad fuels loaded PWR with extended burnups of 18 and 24-months were performed for a steady-state normal operation and selective AOO and DBA scenarios. In general, FeCrAl clad fuel showed better performance within safety parameters of interest, such as PCT, DNBR, fuel cladding failure, hydrogen generation, and oxidation rate. A four-loop Westinghouse PWR model was used in the RELAP5-3D system safety analysis simulation along with a power history module to model burnup cycles that generate decay heat power based on the length of the burnup and operational period. Metal-water reaction and cladding deformation models were also used to study fuel cladding integrity during the accident. During the steady-state normal operation, no specific issue was observed. A total of five DBA scenarios were studied, and compared with Zion NPP FSAR data which is available to verify if the simulation correctly represents the scenario. Table 21 shows the summary of each safety analysis case, focusing on the behavior of the major safety parameters. Fuel failure was observed during an LBLOCA for both Zr and FeCrAl cladding and 18 and 24-month burnup cases since the late activation of the ECCS made a similar situation to a recovered LBLOCA scenario.

Table 21. Summary of DBA analysis.

Accident	PCT	DNBR	H_2 Generation	Oxidation	Fuel Failure
Turbine trip	Zr showed peak under limit	Zr showed peak	Negligible in FeCrAl	Negligible in FeCrAl	None
SBLOCA	All below limit	Agree with FSAR	Negligible in FeCrAl	Negligible in FeCrAl	None
MSLB	All below limit	Agree with FSAR	Negligible in FeCrAl	Negligible in FeCrAl	None
SGTR	Zr showed peak above limit	Zr showed peak but not in FeCrAl	Negligible in FeCrAl	Negligible in FeCrAl	None
LBLOCA	All below limit	Agree with FSAR and Zr showed peak below limit	Negligible in FeCrAl	Negligible in FeCrAl	Occurred from T + 63~68 sec

A recovered LBLOCA scenario was simulated with a severe accident analysis code MELCOR and an environmental consequence analysis code MACCS. The Zion NPP scenario was selected from NRC's SOARCA report. Since Zion NPP reactor core specifications are not publicly available, WBN-1 NPP was used which has similar configurations with Zion NPP. A reactor core was designed with a total of 193 fuel assemblies which has 17×17 lattice configuration for both Zr and FeCrAl clad fuels. SCALE code was used to calculate decay heat and fission product inventories of both 18 and 24 month cycle cases. A Python script was developed to convert data from the MELCOR and MACCS simulation output to generate the accurate volatile behavior of I, Cs, and Mo.

The uncertainties in source term analysis was analyzed based on the propagation of five parameters which mainly affect the core damage, hydrogen generation, and source term release: oxidation start temperature (K), breakaway oxidation start temperature (K), rod burst temperature (K), CsI group fraction in the fuel gap (%) and Xe group fraction in the fuel (%). A stochastic code RAVEN was used to propagate uncertainties with the Monte Carlo method. Comparing Zr and FeCral clad fuel with 18 month burnup cycle, Zr clad fuel cases generally showed higher value in core damage, hydrogen generation and total source term. A strong correlation was found between the breakaway oxidation start temperature and hydrogen generation. Slower breakaway oxidation characteristics of FeCrAl cladding generates significantly smaller amounts of hydrogen compared to Zr cladding.

The environmental consequence analysis was focused on the latent health effect (e.g., cancer fatality), long (up to 50 years) and short (2 hours) term dose and economics analyses. The MACCS input used the default

values of meteorology, site and food data. For the atmosphere plume modeling, the Latin hypercube sampling method was applied for the probabilistic assessment. The analysis includes two different FeCrAl claddings (e.g., APMT and C26M) and Zr clad fuels with both 18 and 24 months fuel cycles. Table 22 shows the summary of environmental consequence analysis. In general, Zr clad fuel 18 months fuel cycle case showed highest value in all consequences which shows even higher than FeCrAl 24 months cases.

Table 22. Summary of environmental consequence analysis.

Consequence	FeCrAl 24 month APMT	FeCrAl 24 month C26M	FeCrAl 18 month APMT	FeCrAl 18 month C26M	Zr 18 month
Max. fatality (person)	8.79	11.1	4.77	4.78	20.3
Max. long term dose (p-Sv)	153	193	82.8	82.9	352
Max. short term dose (p-Sv)	1.08E-3	1.09E-3	9.81E-4	9.08E-4	2.14E-3
Max. cost ($)	5.97E7	7.26E7	3.75E7	2.57E7	7.59E7

Future work will include safety analysis of a PWR loaded with higher enriched Cr-coated Zr ATF during a LBLOCA considering fuel deposition and impacts from the radioactivity release.

6. REFERENCES

[1] Choi, Y.-J. et al. 2022. "Safety Analysis for Accident-Tolerant Fuels with Increased Enrichment and Extended Burnup." INL/RPT-22-68581, Rev. 1, Idaho National Laboratory.

[2] U.S. NRC. 2021. "Standard Review Plan for the Review of Safety Analysis Reports for Nuclear Power Plants: LWR Edition." NUREG-0800. https://www.nrc.gov/reading-rm/doc-collections/nuregs/staff/sr0800/index.html.

[3] U.S. NRC. 1995. "Accident Source Terms for Light-Water Nuclear Power Plants." NUREG-1465. https://www.nrc.gov/reading-rm/doc-collections/nuregs/staff/sr1465/index.html.

[4] Yoon, S., C. Parisi, and Y-J. Choi. 2022. "Assessment of Modeling and Simulation Technical Gaps in Safety Analysis of High-Burnup Accident-Tolerant Fuels." INL/RPT-23-70844, Idaho National Laboratory.

[5] U.S. NRC. 1978. "Standard Format and Content of Safety Analysis Reports for Nuclear Power Plants, LWR Edition." Regulatory Guide 1.70, Revision 3. https://www.nrc.gov/docs/ML0113/ML011340122.html.

[6] American Nuclear Society (ANS). 1983. "Nuclear Safety Criteria for the Design of Stationary Pressurized Water Reactor Plants." ANSI/ANS-51.1-1983. https://www.osti.gov/biblio/6904289.

[7] U.S. NRC. 2014. "MELCOR Best Practices as Applied in the State-of-the-Art Reactor Consequence Analyses (SOARCA) Project." NUREG/CR-7008. https://www.nrc.gov/docs/ML1423/ML14234A136.pdf.

[8] U.S. NRC. 1999. "10 CFR 50.67, Accident Source Term." https://www.nrc.gov/reading-rm/doc-collections/cfr/part050/part050-0067.html.

[9] Choi, Y-J., et al. 2021. "Demonstration of the Plant Fuel Reload Process Optimization for an Operating PWR." INL/EXT-21-64549, Idaho National Laboratory.

[10] Commonwealth Edison Company. 1993. "Zion Station Updated Final Safety Analysis Report."

[11] Idaho National Laboratory. 2018. "RELAP5-3D© Code Manual Volume 1: Code Structure, System Models and Solution Methods." INL/MIS-15-36723, Revision 4.4, Idaho National Laboratory (Limited access to data license holders).

[12] Zhang, H., C. Parisi, H. Zhang, D. Mandelli, C. Blakely, J. Yu, R. Youngblood, et al. 2018. "Plant-Level Scenario-Based Risk Analysis for Enhanced Resilient PWR – SBO and LBLOCA." INL/EXT-1851436, Idaho National Laboratory. https://doi.org/10.2172/1495192.

[13] Lewis, E. E. 1979. *Nuclear Power Reactor Safety*. John Wiley & Sons, ISBN978-0471533351, https://doi.org/10.13182/NT79-A32389.

[14] OECD/NEA. 2009. "Nuclear Fuel Behaviour in Loss-of-coolant Accident (LOCA) Conditions State-of-the-art Report." ISBN 978-92-64-99091-3.

[15] OECD/NEA. 1999. "Pressurised Water Reactor Main Steam Line Break (MSLB) Benchmark - Volume I, Volume I: Final Specifications." https://www.oecd-nea.org/jcms/pl_13242/pressurised-water-reactor-main-steam-line-break-mslb-benchmark-volume-i.

[16] U.S. NRC. 1996. "Steam Generator Tube Failures." NUREG/CR-6365. https://doi.org/10.2172/236258.

[17] U.S. NRC. 1988. "Risk Assessment of Severe Accident-Induced Steam Generator Tube Rupture." NUREG-1570. https://doi.org/10.2172/582237.

[18] F. J. Erbacher and S. Leistikow. 1985. "A Review of Zircaloy Fuel Cladding Behavior in a Loss-of-Coolant Accident." KFK-3973, Institut für Materialforschung and Institut für Reaktorbauelemente. https://doi.org/10.5445/IR/270021792.

[19] "RAVEN." https://raven.inl.gov/SitePages/Overview.aspx

[20] U.S. NRC. 2021. "Setpoints for Safety-Related Instrumentation." Regulatory Guide 1.105.

[21] Le Saux, M., J.-C. Brachet, V. Vandenberghe, A. Ambard, and R. Chosson. 2020. "Breakaway oxidation of zirconium alloys exposed to steam around 1000°C." *Corrosion Science* 176. https://doi.org/10.1016/j.corsci.2020.108936.

[22] Huber, F. 2018. *A Logical Introduction to Probability and Induction*. New York: Oxford University Press. ISBN 9780190845414.

[23] Pint, B. A. 2012. "High temperature oxidation of fuel cladding candidate materials in steam–hydrogen environments." *Journal of Nuclear Materials* 440: 420-427. https://doi.org/10.1016/j.jnucmat.2013.05.047.

[24] Goodson C. E., and Geelhood K. J. 2020 "Degradation and Failure Phenomena of Accident Tolerant Fuel Concepts – FeCrAl Alloy Cladding." PNNL-30445, Pacific Northwest National Laboratory. https://www.nrc.gov/docs/ML2027/ML20272A218.pdf.

[25] Salay, M., Corson, J., and Campbell S. 2021. "FFRD Impact on the Containment Source Term." U.S. NRC. https://www.nrc.gov/docs/ML2119/ML21197A069.pdf.

[26] Wilks, S. S. 1941. "Determination of Sample Sizes for Setting Tolerance Limits." *Annals of Mathematical Statistics* 12(1): 91–96. https://doi.org/10.1214/aoms/1177731788.

[27] Choi, Y-J. and C. Parisi. 2021. "Risk-Informed Multi-Physics Best-Estimate Plus Uncertainties (BEPU): Demonstration of LOCA Scenario-Based Reflood Phenomena." INL/EXT-21-64450, Idaho National Laboratory.

[28] Park, K. I. 2018. *Fundamentals of Probability and Stochastic Processes with Applications to Communications*. Springer. ISBN 978-3-319-68074-3. https://doi.org/10.1007/978-3-319-68075-0.

[29] U.S. NRC. 2022. "Technical Bases for Consequence Analyses Using MACCS (MELCOR Accident Consequence Code System)." NUREG/CR-7270, SAND-2022-12166R, Nuclear Regulatory Commission, Sandia National Laboratory. https://doi.org/10.2172/1898138.

Page intentionally left blank

Appendix A
List of Design-Basis Accidents

Appendix A
List of Design-Basis Accidents

This section lists the DBA categories according to their anticipated frequency of occurrence based on the U.S. NRC's Regulatory Guide 1.70, "Standard Format and Content of Safety Analysis Reports for Nuclear Power Plants, LWR Edition" and the criteria from ANS 18.2-1973, "Nuclear Safety Criteria for the Design of Stationary Pressurized Water Reactor Plants."

A-1. Condition I—Normal Operation and Operational Transients

Conditional I occurrences are those expected frequently or regularly in the course of power operation, refueling, maintenance, or maneuvering of the plant. As such, Condition I occurrences are accommodated with a margin between any plant parameter and the value of that parameter that would require either automatic or manual protective action. Inasmuch as Condition I occurrences occur frequently or regularly, they must be considered from the point of view of affecting the consequences of fault conditions (Conditions II, III, and IV). In this regard, the analysis of each fault condition described is generally based upon a conservative set of initial conditions corresponding to adverse conditions that can occur during Condition I operation.

- Steady-state and shutdown operations

  - Power operation (>5 to 100% of rated thermal power)
  - Startup ($K_{eff} \geq 0.99$, $\leq$ 5% of rated thermal power)
  - Hot standby (subcritical, residual heat removal system [RHRS] isolated)
  - Hot shutdown (subcritical, RHRS in operation)
  - Cold shutdown (subcritical, RHRS in operation)
  - Refueling

- Operation with permissible deviations

  - Operation with components or systems out of service
  - Leakage from fuel with clad defects
  - Radioactivity in the reactor coolant
    - Fission products
    - Corrosion products
    - Tritium
  - Operation with SG leaks up to the maximum allowed by the technical specifications
  - Testing as allowed by the technical specifications

- Operational transients

  - Plant heatup and cooldown (up to 100°F/hour for the RCS, 200°F/hour for the pressurizer [PRZ] during cooldown, and 100°F/hour for the PRZ during heatup)
  - Step load changes (up to ±10%)
  - Ramp load changes (up to 5%/minute)
  - Load rejection up to and including design full load rejection transient.

A-2. Condition II—Faults of Moderate Frequency

Condition II incidents are any one of which may occur during a calendar year for a particular plant (also known as anticipated operational occurrences, AOOs). These faults, at worst, result in a reactor trip with the plant being capable of returning to operation. By definition, these faults (or events) do not propagate to cause a

more serious fault (i.e., Condition III or IV events). In addition, Condition II events are not expected to result in fuel rod failures or RCS, or secondary system over pressurization.

- Feedwater (FW) system malfunctions that result in a decrease in FW temperature

- FW system malfunctions that increase FW flow

- Excessive increase in secondary steam flow

- Inadvertent opening of an SG relief or safety valve

- Loss of external electrical load

- Turbine trip

- Inadvertent closure of main steam isolation valves

- Loss of condenser vacuum and other events resulting in turbine trip

- Loss of nonemergency AC power to the station auxiliaries

- Loss of normal FW flow

- Partial loss of forced reactor coolant flow

- Uncontrolled RCCA bank withdrawal from a subcritical or low-power startup condition

- Uncontrolled RCCA bank withdrawal at power

- RCCA misalignment (dropped assembly, dropped assembly bank, or statically misaligned assembly)

- Startup of an inactive RCP at an incorrect temperature

- Chemical and volume control system (CVCS) malfunction results in a decrease in the boron concentration in the reactor coolant

- Inadvertent operation of the ECCS during power operation

- CVCS malfunction that increases reactor coolant inventory

- Inadvertent opening of a PRZ safety or relief valve

- Break in instrument line or other lines from the RCPB that penetrate containment.

A-3. Condition III—Infrequent Faults

By definition, Condition III occurrences are faults that may occur very infrequently during the life of the plant. They will be accommodated with the failure of only a small fraction of the fuel rods, although sufficient fuel damage might occur to preclude the resumption of the operation for a considerable outage time. The release of radioactivity will not be sufficient to interrupt or restrict public use of those areas beyond the exclusion radius. A Condition III fault will not, by itself, generate a Condition IV fault or result in a consequential loss of function of the RCS or containment barriers.

- Steam system piping failure (minor)

- Complete loss of forced reactor coolant flow

- RCCA misalignment (single RCCA withdrawal at full power)

- Inadvertent loading and operation of a fuel assembly in an improper position

- LOCAs resulting from a spectrum of postulated piping breaks within the RCPB (e.g., small-break LOCA)

- Postulated radioactive ground releases due to liquid tank failures

- Spent fuel cask drop accidents.

A-4. Condition IV—Limiting Faults

Condition IV occurrences are faults that are not expected to take place but are postulated because their consequences would include the potential release of significant amounts of radioactive material. They are the most drastic events that must be designed against and represent limiting design cases. Condition IV faults are not to cause a fission product release to the environment resulting in an undue risk to public health and safety in excess of guideline values of 10CFR100. A single Condition IV fault is not to cause a consequential loss of required functions of systems needed to cope with the fault, including those of the ECCS and containment.

- Steam system piping failure (major)
- FW system pipe break
- RCP shaft seizure (locked rotor)
- RCP shaft break
- Spectrum of RCCA ejection accidents
- SG tube failure
- LOCAs resulting from the spectrum of postulated piping breaks within the RCPB (e.g., large-break LOCA)
- Design-basis fuel handling accidents.

Page intentionally left blank

Appendix B
RELAP5-3D Model For Four-Loop Westinghouse Pressurized Water Reactor

Appendix B
RELAP5-3D Model For Four-Loop Westinghouse Pressurized Water Reactor

Pressurizer Spray Lines

Broken Loop 4

Intact Loop 1

Vessel

Intact Loop 3

Intact Loop 2